Geological Society of America Bulletin

Structural and sedimentological development of footwall growth synclines along an intraforeland uplift, east-central Bighorn Mountains, Wyoming

Richard G. Hoy and Kenneth D. Ridgway

Geological Society of America Bulletin 1997;109;915-935
doi: 10.1130/0016-7606(1997)109<0915:SASDOF>2.3.CO;2

Structural and sedimentological development of footwall growth synclines along an intraforeland uplift, east-central Bighorn Mountains, Wyoming

Richard G. Hoy
Kenneth D. Ridgway* } *Department of Earth and Atmospheric Sciences, Purdue University, West Lafayette, Indiana 47907-1397*

ABSTRACT

Structural, sedimentological, and provenance data from Paleogene synorogenic deposits of the east-central flank of the Bighorn Mountains provide new information about the development of footwall growth synclines, the evolution of fault-related folds, and the erosional unroofing history of intraforeland uplifts. Three conglomerate units, the upper conglomerate member of the Fort Union Formation and the Kingsbury and Moncrief Members of the Wasatch Formation, are incorporated within an asymmetric, east-verging growth syncline in the footwall of the main range-bounding thrust system. Three stages of footwall deformation are recorded within these conglomerates. Analysis of mapped progressive unconformities, retrodeformed balanced cross sections, and conglomerate clast composition data define these stages as part of a continuum of deformation associated with the development of footwall growth synclines.

Development of an anticline-syncline pair marked the earliest stage of growth syncline formation (stage I). Rotation of the shared fold limb resulted in amplification of the growth syncline. Fine-grained, synorogenic sediment derived from easily eroded Mesozoic mudstone bypassed the growth syncline during this stage. By the end of Lebo Shale deposition, an average of 12.1% of shortening and 6.46 km of uplift had occurred along the range margin. Continued growth syncline development was marked by the deposition of the Kingsbury Conglomerate. The Kingsbury Conglomerate was derived from resistant, middle and lower Paleozoic carbonate strata in the uplifted source terrane. Intraformational unconformities, recording as much as 55° of bed rotation, were developed within the Kingsbury Conglomerate as fold limb rotation occurred coeval with deposition. Cross sections indicate that during this early stage of fault-related folding, an average of 16.9% shortening and 8.12 km of uplift occurred along the eastern flank of the Bighorn Mountains (end of stage I). The intermediate stage (stage II) of footwall growth syncline development involved partial truncation of the growth syncline by the advancing thrust faults and deposition of the Moncrief Conglomerate. The lower portion of the Moncrief Conglomerate was rotated basinward in the developing growth syncline. The final stage of deformation (stage III) was dominated by the thrust faulting of middle and lower Paleozoic strata eastward over steeply dipping Mesozoic strata and rotated Eocene synorogenic conglomerate. During this stage of deformation, the Moncrief Conglomerate was deformed, as the initially blind thrusts propagated into the near-surface conglomerate deposits, truncated the entire footwall syncline, and overrode the synorogenic conglomerate package. Cross sections in areas where this final stage of deformation is well developed indicate that an average of 24.1% shortening and 9.7 km of uplift had occurred along the eastern margin of the Bighorn Mountains.

The caliber of synorogenic deposition in the Powder River basin was linked directly to the lithologic composition of the Bighorn Mountains. Approximately half of the 3.6-km-thick source-stratigraphic section of the eastern Bighorn Mountains was eroded prior to accumulation of conglomerate. The majority of this eroded material was derived from Mesozoic mudstone and poorly indurated sandstone that were incapable of generating coarse detritus. The first Paleogene conglomerates deposited along the east-central Bighorn Mountains, therefore, do not represent the initiation of Laramide uplift, but instead represent the exposure of coarse-clast–forming rock types from the lower half of the hanging-wall stratigraphic section (i.e., the Mississippian Madison Limestone and Ordovician Bighorn Dolomite).

INTRODUCTION

For over a decade, there has been increasing interest in the relationship between thrust fault deformation and synorogenic sedimentation within foreland and intraforeland basins (e.g., Lawton, 1985; Steidtmann and Schmitt, 1988; Heller et al., 1988; Jordan et al., 1988; Lawton et al., 1994; DeCelles and Mitra, 1995). Several studies have shown the importance of using synorogenic deposits in the structural analysis of foreland basins (DeCelles et al., 1991; Burbank et al., 1992a; Burbank and Vergés, 1994). A few studies have integrated both structural data and the provenance of synorogenic conglomerates to better determine the link between thrusting and deposition (Graham et al., 1986; Lawton, 1986; Pivnik, 1990; DeCelles et al., 1991). Several recent studies have also recognized the development of footwall growth synclines adjacent to major thrust faults as a characteristic structural element (DeCelles et al., 1987, 1993; Vergés et al., 1996; Ridgway et al., 1997). Footwall growth synclines, as defined here, are footwall folds in which sedimentation took place during structural growth of the syncline. Footwall growth synclines have been interpreted as forming in response to fault-propagation folding (Suppe and Medwedeff, 1990; DeCelles et al., 1991), fault-bend folding (Medwedeff, 1989), and detachment folding (Hardy and Poblet, 1994; Vergés et al., 1996; Espina et al., 1996). The presence of rotated strata, progressive unconformities, and abrupt changes in conglomerate clast composition, documented within growth synclines, attests to the dynamic relationship between thrust fault deformation, fold development, and synorogenic sedimentation.

One goal of this study is to develop a better understanding of the structural evolution of footwall growth synclines associated with fault-related folds. The east-central Bighorn Mountains, deformed by west-dipping thrust faults (Fig. 1), are a natural laboratory for studying the evolution of growth synclines. Here, synorogenic conglomerates in the upper conglomerate member of the Paleocene Fort Union Formation and in the Kingsbury

*E-mail: ridge@omni.cc.purdue.edu

GSA Bulletin; August 1997; v. 109; no. 8; p. 915–935; 16 figures; 1 table.

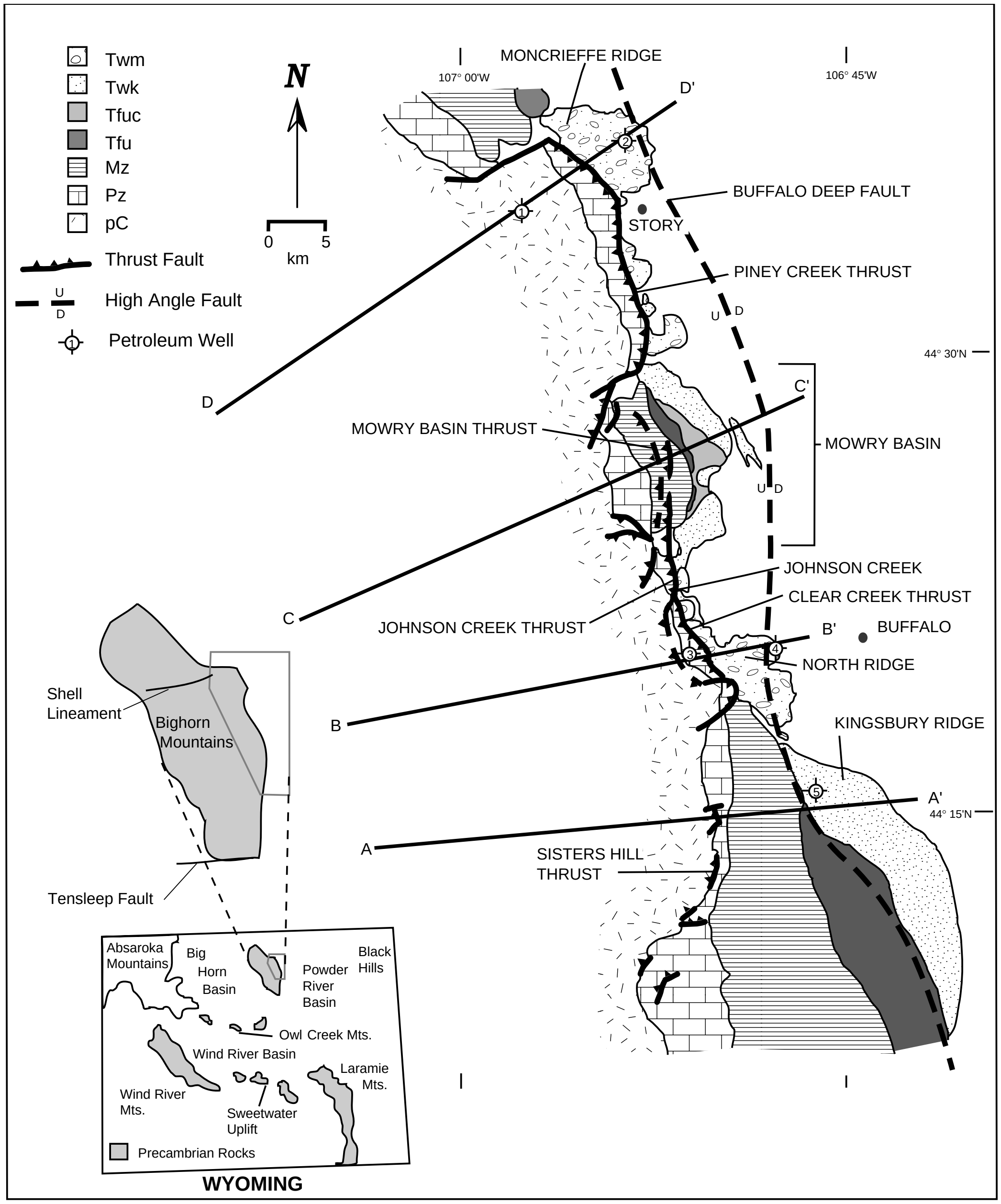

Figure 1. General geologic map of the east-central flank of the Bighorn Mountains, Wyoming, showing major structural features and location of the study area (Hose, 1955; Mapel, 1959). This part of the range can be subdivided into four structural units (from north to south): Piney Creek thrust block, Mowry basin, Clear Creek thrust, and Kingsbury Ridge. Paleozoic strata (block pattern) crop out as flatirons along the range margin. Mesozoic strata (striped pattern) are exposed in the Mowry basin and at Kingsbury Ridge. Lines A–A′, B–B′, C–C′, and D–D′ indicate locations of cross sections shown in Figures 6, 9, 11, and 12. Location of petroleum wells with geophysical logs used for this study: 1—Granite Ridge #1-2-9D; 2—Granite Ridge velocity test hole; 3—Arco Kenny Ranch well #1-4; 4—Buffalo Federal 1-1 well; 5—Mapco I-30 Federal well.

and Moncrief Members of the Eocene Wasatch Formation have been incorporated within an asymmetric east-verging growth syncline along the main range-bounding thrust fault system (Figs. 1 and 2) (Ridgway et al., 1992; Hoy and Ridgway, 1995). Mapping of progressive unconformities within this footwall growth syncline and conglomerate compositional data provide constraints needed for retrodeforming balanced cross sections that delineate the various stages of fault-related fold development.

Another goal of this study is to closely document the uplift and unroofing history of an intraforeland uplift and associated sediment deposition within the adjacent basin. Many recent studies have shown that coarse-grained deposition in foreland and intraforeland basins may be controlled by a number of interacting variables (e.g., Flemings and Jordan, 1990). In some cases, conglomerate deposition has been attributed mainly to uplift on nearby thrust sheets (Burbank et al., 1988; Steidtmann and Middleton, 1991; Jordan et al., 1993; DeCelles, 1994; Pivnik and Khan, 1996). In other cases, the rate of basin subsidence has been proposed as the controlling factor on synorogenic conglomerate deposition (Beck et al., 1988; Heller et al., 1988; Burbank et al., 1992b; Heller and Paola, 1992). Results of our study in the Bighorn Mountains indicate that an additional variable, the lithologic composition of the intraforeland uplift, had an important influence on the caliber of synorogenic sediment deposited in the adjacent basin.

STRUCTURE AND PRE-LARAMIDE STRATIGRAPHY OF THE BIGHORN RANGE

The Bighorn Mountains of north-central Wyoming and south-central Montana (Fig. 1) are part of the Laramide Rocky Mountain foreland (see Brown, 1988, for a review). The Bighorn Mountains are an asymmetric, basement-cored uplift and form the western margin of the Powder River basin. Demorest (1941) subdivided the range into three segments on the

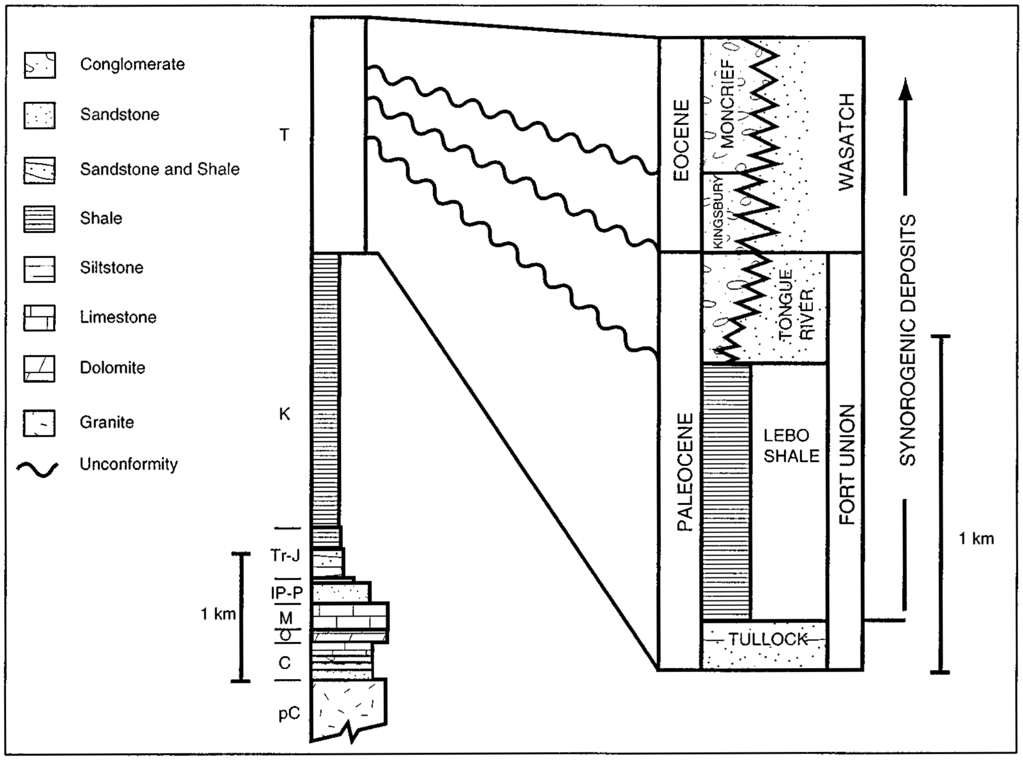

Figure 2. Stratigraphic column of the western Powder River basin and east-central Bighorn Mountains. Pre-Laramide strata (pC-K)–Precambrian (pC): granite and gneiss; Cambrian (C): Flathead Sandstone (locally quartzitic, 105 m) and Gros Ventre Formation (195 m); Ordovician (O): Bighorn Dolomite (110 m); Mississippian (M): Madison Limestone (190 m); Pennsylvanian–Permian (IP-P): Pennsylvanian Amsden and Tensleep Formations (75 and 83 m, respectively), Permian Goose Egg Formation (55 m); Triassic–Jurassic (Tr-J): Triassic Chugwater Formation (240 m), Jurassic Gypsum Spring (50 m), Sundance (85 m), and Morrison Formations (55 m); Cretaceous (K): Cloverly Formation (45 m), Skull Creek Shale (50 m), Newcastle Sandstone (15 m), Mowry Shale (160 m), Frontier Formation (150 m), Cody Shale (1080 m), Parkman Sandstone (220 m), Bearpaw Shale (60 m), and Lance Formation (580 m). Tertiary synorogenic strata (T): Paleocene Fort Union Formation (Tullock, Lebo Shale, and Tongue River Members; 360–1180 m) and Eocene Wasatch Formation (Kingsbury and Moncrief Conglomerate Members; 300–910 m). Thickness of individual synorogenic conglomerates discussed in text: Fort Union conglomerate (430 m), Kingsbury Conglomerate (240 m), and Moncrief Conglomerate (430 m). Thickness data from Hose (1955) and Mapel (1959).

basis of the configuration of dominant structural features. Uplift in the northern and southern segments of the range was controlled by west-verging thrust faults, whereas the central segment, delineated by the Tensleep fault on the south and the Shell lineament on the north, was controlled by east-verging faults (Fig. 1). Initial geologic mapping (Darton, 1906; Demorest, 1941; Hose, 1955; Mapel, 1959) identified the major faults and subdivided the east-central flank of the range into four structural units. These are (from north to south) the Piney Creek thrust block, the Mowry basin, the Clear Creek thrust, and Kingsbury Ridge (Fig. 1). Two roughly north-south–striking fault systems are present along the east-central flank of the Bighorn Mountains. The western fault is the Bighorn fault, but different names have been applied to this fault in each of the subdivisions: the Piney Creek thrust, the Mowry basin thrust, the Johnson Creek and Clear Creek thrusts, and the Sisters Hill thrust at Kingsbury Ridge (Fig. 1). The eastern fault, identified in seismic sections by Foster et al. (1969) and later named the Buffalo Deep fault by Blackstone (1981), roughly parallels the range margin (Fig. 1). This fault has been interpreted as a reactivated basement fault with as much as 1.2 km of displacement (Foster et al., 1969).

Initial interpretations of the structures along the east-central part of the Bighorn Mountains proposed thrust faulting as the dominant uplift mechanism (Demorest, 1941). Later studies suggested a block-uplift mechanism as the primary deformational style, particularly along the Piney Creek thrust (Palmquist, 1978; Stearns, 1978). Seismic surveys (Foster et al., 1969; Robbins and Grow, 1990) and wells drilled through the Precambrian rocks in the hanging wall of the Bighorn thrust have demonstrated that the central part of the range is structurally controlled by east-verging, relatively shallow dipping thrust faults (approximately 30°W). More recent studies have interpreted horizontal compression as the primary deformational agent (Blackstone, 1981; Jenkins, 1986; Brown, 1988; Hudson, 1992; Stone, 1993).

The pre-Laramide stratigraphy of the Bighorn Mountains can be divided into three general rock types: Precambrian granite and gneiss, lower and middle Paleozoic carbonate strata (610 m), and upper Paleozoic and Mesozoic mudstones (3020 m) (Hose, 1955; Mapel, 1959) (Fig. 2). The thickest formations in the lower and middle Paleozoic carbonate package are the Ordovician Bighorn Dolomite (110 m) and the Mississippian Madison Limestone (190 m). The thickest formation in the upper Paleozoic and Mesozoic package is the Cretaceous Cody Shale (1080 m) (Fig. 2).

STRATIGRAPHY AND SEDIMENTOLOGY OF SYNOROGENIC DEPOSITS OF THE POWDER RIVER BASIN

The Powder River basin is one of several nonmarine intraforeland basins that formed in response to basement deformation during the Laramide orogeny (Dickinson et al., 1988). The lower Tertiary fill of the Powder River basin is more than 2000 m thick and consists of the Paleocene Fort Union Formation and the Eocene Wasatch Formation. The Fort Union Formation has three members: the early Paleocene Tullock Member, the middle Paleocene Lebo Shale, and the late Paleocene Tongue River Member (Fig. 2) (Hose, 1955; Mapel, 1959). The Wasatch Formation has two members: the Kingsbury Conglomerate and the Moncrief Conglomerate (Fig. 2). The two formations contain three synorogenic conglomerates, the upper conglomerate member of the Paleocene Fort Union Formation (Tongue River equivalent), and the Kingsbury and the Moncrief conglomerates (Fig. 2). These conglomerates are located along the western flank of the Powder River basin adjacent to the central segment of the Bighorn Mountains (Fig. 1) (Sharp, 1948; Obernyer, 1979). They have been interpreted as alluvial-fan deposits (Sharp, 1948; Obernyer, 1979), and contain proximal fan, medial fan, and distal fan facies (Flores and Warwick, 1984; Ridgway et al., 1991).

Isopach data indicate that initiation of the Powder River basin as a structural and depositional basin occurred during deposition of the middle Paleocene Lebo Shale (Curry, 1971; Ayers, 1986). Several studies have shown that basin subsidence was greatest adjacent to the thrusted east-central segment of the Bighorn Mountains (Curry, 1971; Obernyer, 1979; Ayers, 1986; Flores, 1986), where the Lebo Shale and Tongue River Members of the Fort Union Formation and the Wasatch Formation are thickest. Depositional environments during Fort Union and Wasatch deposition were predominantly alluvial fan, fluvial, and lacustrine (Seeland, 1976; Ethridge et al., 1981; Flores and Hanley, 1984; Ayers, 1986; Weaver and Flores, 1987). Major Paleocene and Eocene fluvial systems flowed northward through the Powder River basin toward the Williston basin (Flores and Ethridge, 1985).

METHODS

Sedimentological data collected from the three Tertiary conglomerate units along the western edge of the Powder River basin include conglomerate clast composition, paleocurrent directions, and maximum particle size. These data were collected within the context of measured stratigraphic sections. Structural data used for construction of cross sections were collected on traverses perpendicular to the range margin. These data include orientations of bedding units and faults in the Paleozoic and Mesozoic strata in the hanging wall of range-bounding thrusts and also in the footwall synorogenic Tertiary strata. Angular unconformities separating the three conglomerates were mapped at a scale of 1:24 000 and the amount of discordance was measured. This information, along with data obtained from petroleum well logs, was used to construct four balanced cross sections. The cross sections were both line and area balanced using the standard methods established by Dahlstrom (1969) and Woodward et al. (1985).

Each cross section was sequentially retrodeformed to show the relative positions of the hanging wall and footwall during the various stages of synorogenic deposition. Assuming a 10° depositional slope for the proximal sections of the currently rotated alluvial-fan deposits, the strata can be restored and the approximate structural level of the feeder canyon can be projected into the hanging-wall stratigraphy. This projection delineates which stratigraphic units were exposed on the hanging wall of the thrust fault, and, therefore, which rock types were available as source rocks for the synorogenic deposits in the Powder River basin during each stage of deformation. Each interformational and intraformational angular unconformity mapped in the synorogenic conglomerates was restored in a similar fashion during the retrodeformation process. The match between measured conglomerate clast composition in the footwall and the possible source stratigraphic section (based on projection into the hanging wall) helped determine geologically plausible solutions during each stage of retrodeformation. This method is similar to that developed by DeCelles et al. (1991) in their study of the Beartooth Conglomerate of Wyoming and Montana.

Pinning point locations for the cross sections were chosen in the following manner. The eastern pinning point in the footwall was located in the undeformed Powder River basin, close to the basin axis. Because the majority of rocks exposed in the hanging wall are Precambrian crystalline basement, there is no easily chosen location for the western pinning points based on stratigraphy. To find a western pinning point, the Paleozoic sedimentary sections were projected from bedding attitudes on both flanks of the range until the hinge of the fold was determined. Assuming concentric flexural-slip folding where no slip occurs between units at the hinge, this location was used as the western pinning point for each of the cross sections.

Balancing of the cross sections was based upon three assumptions. First, it is assumed that all uplift along the current trend of the Bighorn Mountains occurred during the Laramide orogeny. Central Wyoming has certainly undergone earlier and later episodes of deformation, but on the basis of previous tectonic studies of the Bighorn Mountains (Demorest, 1941; Hoppin, 1961; Curry, 1971; Jenkins, 1986), these other deformational events had little influence on the present structural configuration. The second assumption is that the climatic controls on weathering of the source section did not significantly alter the composition of detritus transported and deposited in the basin. Despite the interpretation that the Paleogene synorogenic conglomerates were deposited by wet alluvial fans (Flores and Warwick, 1984), and that the annual temperature increased from 10 °C at 58.5 Ma to 18 °C at 50.5 Ma (Hickey, 1980; Wing et al., 1991), the consistent abundance of pebble- to cobble-sized limestone clasts within the synorogenic deposits indicates that chemical weathering was not a controlling factor. The third assumption is that very little longitudinal transport of sediment occurred in the alluvial-fan systems. Paleocurrent data from this and previous studies (Flores and Ethridge, 1985; Flores, 1986) support this assumption. Therefore, we would not expect conglomerate clasts derived from adjacent erosional drainages along strike to significantly influence clast composition data at a given locality.

One cross section was constructed through each of the four structural segments of the east-central flank of the range (Fig. 1). Analysis of the stratigraphy, clast composition, and deformation of the synorogenic conglomerates within the framework of cross sections is used to interpret the structural evolution of each segment.

ANALYSIS OF STRUCTURAL EVOLUTION

Kingsbury Ridge

Stratigraphy. Kingsbury Ridge is the type locality of the Eocene Kingsbury Conglomerate (Twk) (Fig. 1). At this location, the Kingsbury Conglomerate is 240 m thick. The conglomerates of this formation are massive, clast-supported units with lenticular geometries (Fig. 3A). Maximum particle size data range from an average of 5–10 cm at the eastern edge of Kingsbury Ridge to 25–30 cm in the west-central part (Fig. 4A). Pebble imbrications indicate that paleoflow was to the east-northeast (Fig. 4A). Matrix-supported conglomerate units interpreted as debris-flow deposits are present, but uncommon, and have an average maximum particle size of 80 cm. Sandstone beds are predominantly massive, but in some cases have interbedded siltstones (Fig. 3A). The Kingsbury Conglomerate in this area has been interpreted as middle to distal alluvial-fan deposits (Flores and Warwick, 1984).

Clast Composition. The composition of the Kingsbury Conglomerate indicates derivation from the Cambrian through Mississippian formations, and a minor contribution from Precambrian sources (Fig. 5A). At the base of the Kingsbury Conglomerate section at Kingsbury Ridge, 80% of the conglomerate composition is Mississippian Madison Limestone (Mm) and Ordovician Bighorn Dolomite (Ob) (Fig. 5A). Approximately 11% of the clasts were derived from Cambrian formations: the flat-pebble conglomerate and purple limestone of the upper Gros Ventre Formation (Cgv), and the Flathead Sandstone (Cf). Precambrian granite and gneiss constitute only 8% of the clast types. At the top of the section, only 30% of the clasts were derived from the Mississippian Madison Limestone and Ordovician Bighorn Dolomite, whereas the Cambrian and Precambrian contribution increased to approximately 68% (43% Cgv and Cf; 25% pC). At the top of the Kingsbury Conglomerate section, 2% of the conglomerate clasts are reworked basal Kingsbury Conglomerate (Twk in Fig. 5A).

Deformation of Synorogenic Conglomerate. Growth strata are well developed in the Kingsbury Conglomerate at Kingsbury Ridge. The con-

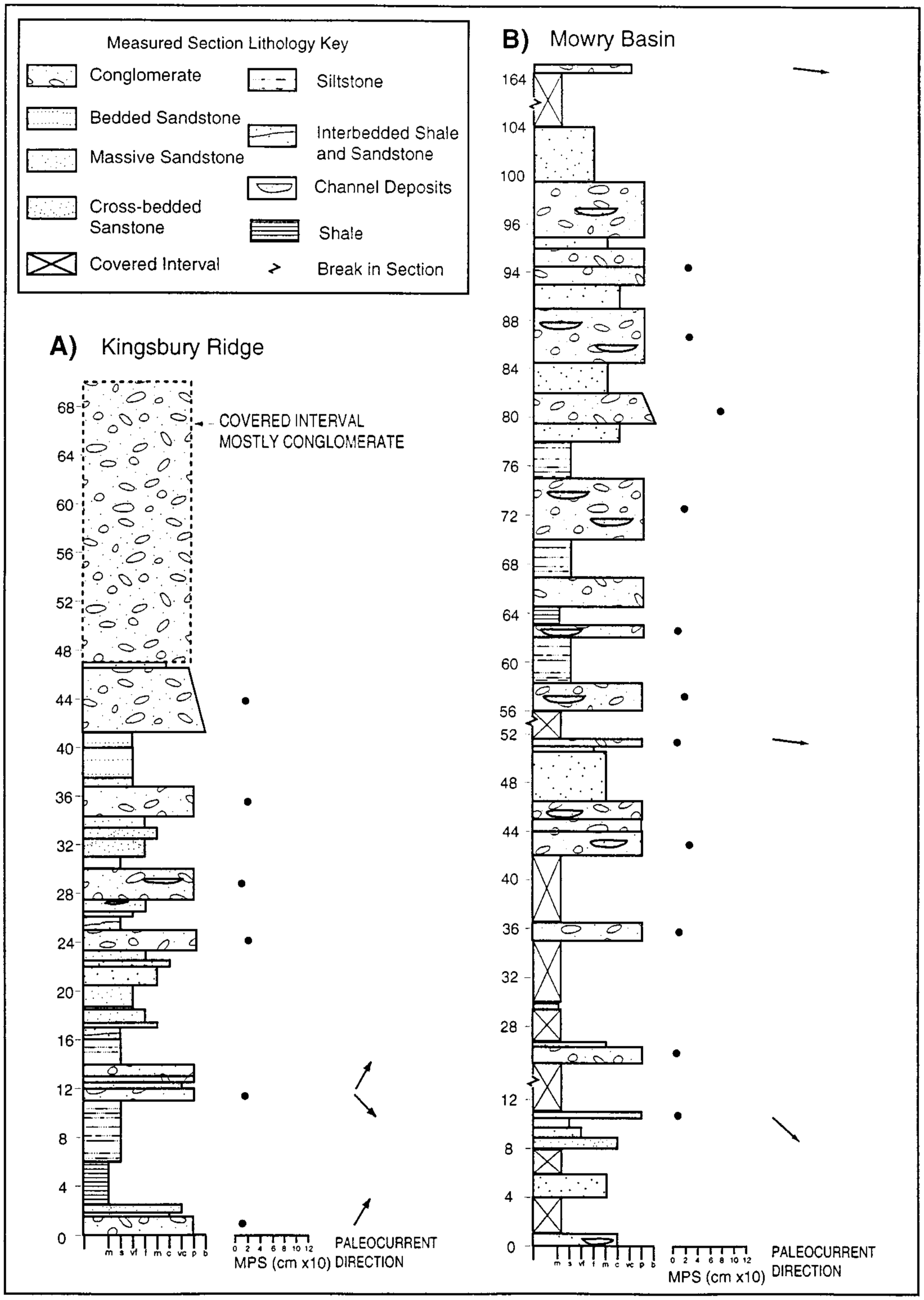

Figure 3. Log of measured stratigraphic sections from the Kingsbury Conglomerate including maximum particle sizes (MPS) and paleocurrent directions. (A) Midfan deposits at Kingsbury Ridge. Location 3A in Figure 4A. (B) Midfan deposits in the Mowry basin. Location 3B in Figure 4C. Grain-size abbreviations: m—mud, s—silt, vf—very fine sand, f—fine sand, m—medium sand, c—coarse sand, vc—very coarse sand, p—pebble, b—boulder. Arrows show paleocurrent directions where north is taken as the top of the figure. Paleocurrent directions from imbricated conglomerate clasts and trough cross-stratification. Note scale changes between individual sections.

tact with the underlying Fort Union deposits is an angular unconformity with as much as 54° of discordance. A traverse perpendicular to the regional strike of the Kingsbury Conglomerate reveals gradual rotation of the strata (Fig. 6C). The steepest dip of the basal Kingsbury Conglomerate is approximately 65°E, whereas deposits at the top of the ridge to the east are dipping about 10°E (Fig. 6C). Assuming an initial 10° depositional slope, the conglomerates have undergone as much as 55° of progressive rotation.

Structural Evolution. Cross section A–A′ shows that two faults, the Sisters Hill thrust (SHT in Fig. 6) on the west and the Buffalo Deep fault (BDF in Fig. 6) on the east, controlled the deformation observed at Kingsbury Ridge. The Mapco I-30 Federal well (well #5 in Figs. 1 and 6) provided control for the footwall stratigraphy. Uplift calculated from cross section A–A′ at the Precambrian-Phanerozoic contact is 8.10 km, and shortening is calculated as 5.73 km (15.5%) (Fig. 6C). Cross section A–A′ was retrodeformed in three stages. (1) Initial uplift of the Bighorn Range occurred along

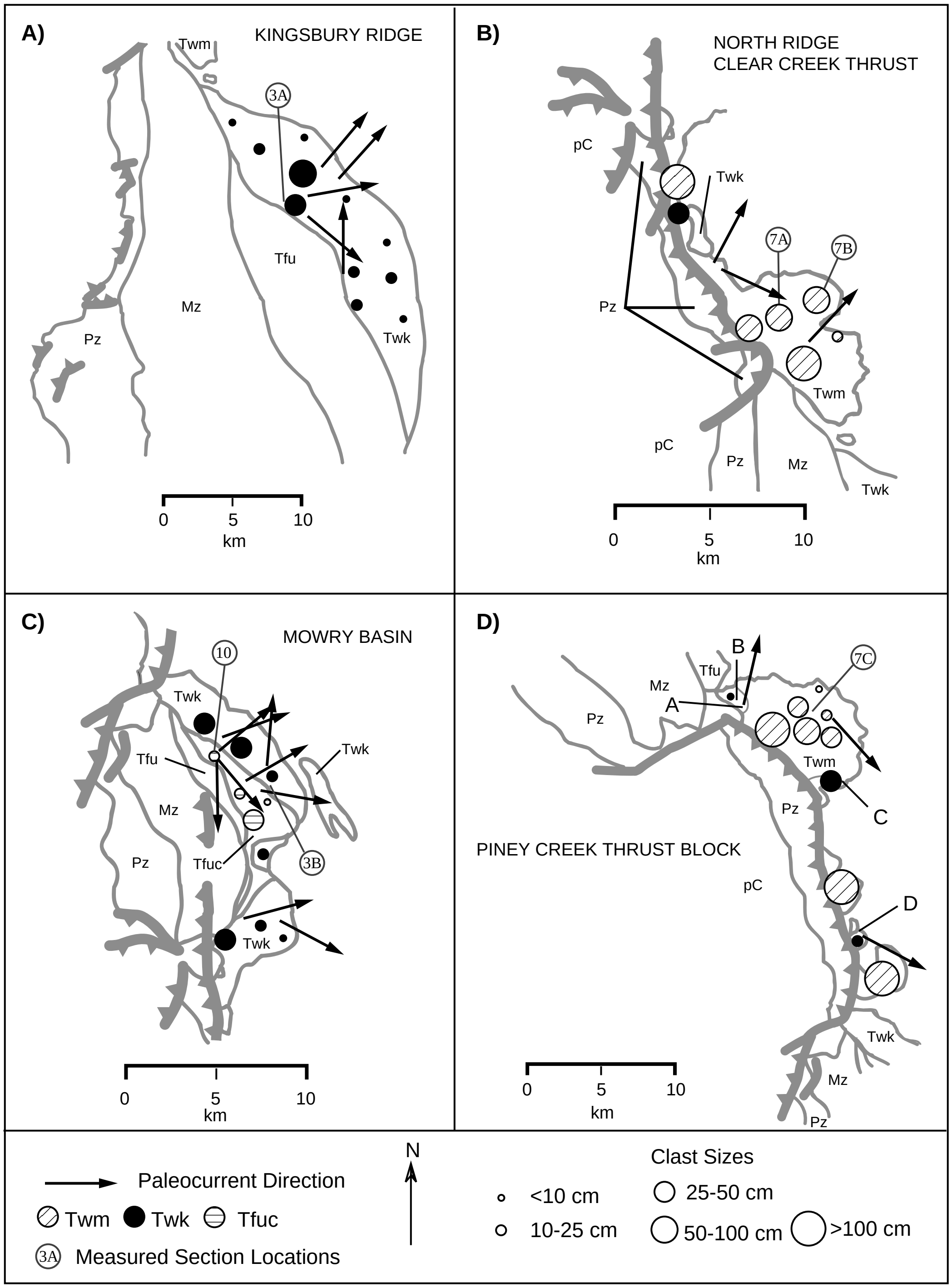

Figure 4. Sedimentologic data of synorogenic conglomerates from each of the four regions in the study area (Fig. 1). Data include the average maximum particle sizes (MPS, dots) and average paleocurrent directions (arrows) from imbricated conglomerate clasts (average measurement of 10 imbricated clasts per station) and trough cross-stratification. Circles containing numbers show location of measured stratigraphic sections. The letters in D represent locations of conglomerate clast compositions shown in Figure 5D. pC—Precambrian crystalline basement; Pz—Paleozoic strata; Mz—Mesozoic strata; Tfu—Fort Union Formation; Tfuc—Fort Union conglomerate; Twk—Kingsbury Conglomerate; Twm—Moncrief Conglomerate.

the Sisters Hill thrust (Fig. 6A). This uplift exposed the easily eroded Mesozoic and upper Paleozoic mudstones (Fig. 2), which are interpreted as the source terrane for the Lebo Shale Member of the Fort Union Formation. Because displacement on the Sisters Hill thrust is approximately 300 m, uplift associated with this fault cannot account for the unroofing of the entire section of Mesozoic rocks (approximately 2 km) or the thickness of the Lebo Shale (915 m). Uplift at the end of movement along the Sisters Hill thrust was 1.85 km with 0.73 km of shortening (2.0%) (Fig. 6A). At this time, most sediment eroded from the hanging wall bypassed the proximal region of the basin. (2) Thrust displacement was transferred from the Sisters Hill thrust to the Buffalo Deep fault (Fig. 6B). The Buffalo Deep fault is interpreted to be part of a large fault-related fold. Its high angle may be indicative of reactivation of a basement fault (Foster et al., 1969), but its expression in the Phanerozoic units between the two range bounding faults is that of a large hanging-wall anticline. This anticline is in part derived from a basement fault (FS1 in Fig. 6), which is a splay of the Buffalo Deep fault. During displacement on FS1, the hinge of this anticline migrated to the west (e.g., rolling-hinge model of Schmidt et al., 1993). The initiation of uplift on

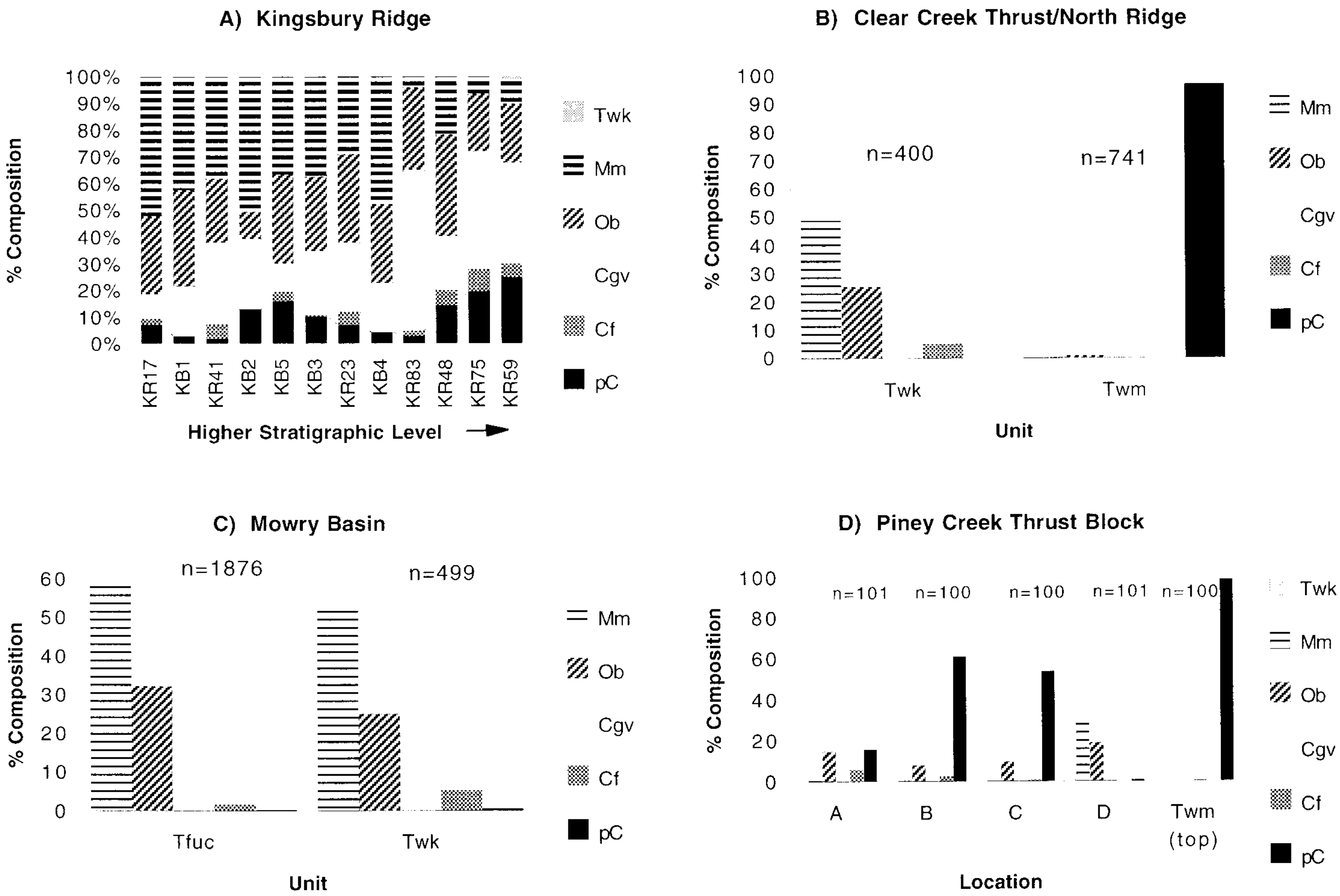

Figure 5. Histograms of conglomerate clast compositions in the four regions of the study area. (A) Upsection change in composition of the Kingsbury Conglomerate at Kingsbury Ridge. Note the decrease in Mississippian Madison Limestone (Mm) and the increase in Cambrian Gros Ventre (Cgv) and Precambrian basement clasts (pC) upsection. Cf—Cambrian Flathead, Ob—Bighorn Dolomite, Twk—reworked Kingsbury Conglomerate clasts. (B) Average clast composition of the Kingsbury Conglomerate (Twk) and Moncrief Conglomerate (Twm) exposed at North Ridge along the Clear Creek thrust and at Johnson Creek. n—number of clasts identified. (C) Average composition of the Fort Union conglomerate (Tfuc) and Kingsbury Conglomerate (Twk) in the Mowry basin. Note the greater contribution of clasts from the Cambrian Gros Ventre (Cgv) and Cambrian Flathead (Cf) Formations in the Kingsbury Conglomerate relative to the Fort Union conglomerate. (D) Composition of the conglomerate outcrops A–D along the Piney Creek thrust block. See Figure 4D for outcrop locations. Note that the compositions are intermediate between those of the Kingsbury Conglomerate and those of the Moncrief Conglomerate exposed elsewhere along the range margin. Compositions of conglomerates at top of Moncrieffe Ridge (Twm) are shown for comparison.

the Buffalo Deep fault allowed for continued exposure and unroofing of the nonresistant Mesozoic and upper Paleozoic units (deposited as the Lebo Shale) until the more durable middle and lower Paleozoic carbonate rocks were exposed in the hanging wall. Initial exposure of the Mississippian Madison Limestone and Bighorn Dolomite marked the onset of Kingsbury Conglomerate deposition; calculated uplift is 6.55 km and shortening is 2.13 km (5.8%) (Fig. 6B). During this stage of deformation, further development of the growth syncline allowed for sediment deposition in the footwall of the Buffalo Deep fault (Fig. 6B). Incorporation of fine-grained Fort Union deposits into the steep limb of the footwall growth syncline, prior to deposition of the Kingsbury Conglomerate, resulted in 54° of angular discordance between the two units. (3) As displacement on the Buffalo Deep fault proceeded, uplift and shortening in the region increased, causing deeper incision into the hanging wall. Deeper hanging-wall dissection is reflected in the Kingsbury Conglomerate clast composition by an upsection increase in Precambrian and Cambrian clast types and a decrease in Mississippian clast types (Fig. 5A). With continued deformation, proximal Kingsbury Conglomerate deposits were incorporated into the steeply dipping western limb of the growth syncline (Fig. 6C). The proximal Kingsbury Conglomerate on the steep limb of the growth syncline became a source of sediment for younger Kingsbury Conglomerate strata being deposited in the hinge of the growing footwall syncline. This cannibalization is documented by the introduction of conglomerate clasts of the Kingsbury Conglomerate into younger Kingsbury Conglomerate deposits (Fig. 5A). With continued rotation of the western limb of the growth syncline, progressive unconformities developed in the Kingsbury Conglomerate; 55° of syndepositional bed rotation occurred within the Kingsbury Conglomerate during this stage of deformation.

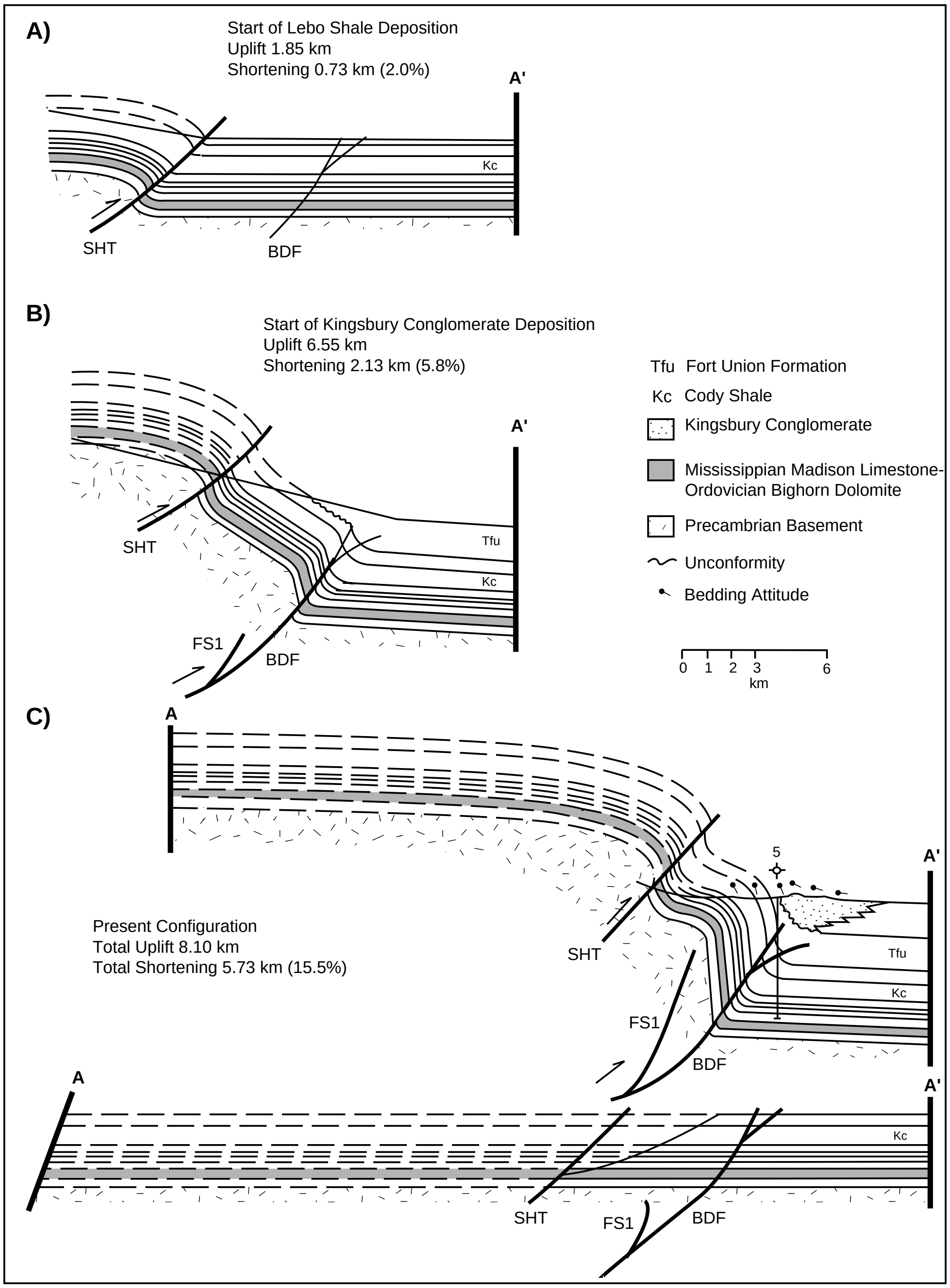

Figure 6. Sequential restoration of cross section A–A′ at Kingsbury Ridge (see Fig. 1 for location of cross section). Amount of uplift and shortening is shown for each stage of retrodeformation. (A) Initial displacement along the Sisters Hill thrust (SHT) and beginning of Lebo Shale deposition in the Powder River basin. (B) Transfer of displacement to the Buffalo Deep fault (BDF) and onset of Kingsbury Conglomerate deposition. Note the development of the footwall growth syncline by this stage. (C) Present structural configuration of Kingsbury Ridge. Note the progressive decrease in dip within the Kingsbury Conglomerate. Petroleum well logs used for construction: 5—Mapco I-30 Federal well. Surface data from Hoy (1996).

Clear Creek Thrust–North Ridge

Stratigraphy. Boulder conglomerates exposed west of Buffalo, Wyoming, are part of a large Eocene alluvial fan system (Sharp, 1948; Nelson, 1968). The deposits are exposed along Clear Creek and along U.S. Highway 16 at North Ridge (Fig. 1). This ancient fan system is composed of the Moncrief Member of the Wasatch Formation (Twm) and is about 430 m thick. The proximal deposits of the Moncrief Conglomerate are clast-supported, boulder conglomerates that are predominantly massive, although upward fining is evident in some units. Mid-fan deposits are composed of thick, upward-fining cobble conglomerate beds with thin interbeds of coarse sandstone (Fig. 7A). The more distal sandstone deposits are finer grained and show evidence of channeling (Fig. 7B). Maximum particle size data in the proximal deposits range from about 20 cm near the base of the section to as much as 400 cm near the top of the section (Fig. 4B). Due to the large, rounded clasts, imbrication is not well developed in the proximal deposits; however, the distal deposits show paleocurrent directions ranging from northeast to southeast (Fig. 4B).

Clast Composition. The clast composition of the Moncrief Conglomerate shows that the majority of the clasts were derived from Precambrian gneiss and granite (Fig. 5B). The conglomerate composition indicates that even at the onset of Moncrief deposition, the source terrane was composed predominantly of Precambrian rocks. Along the line of cross section B–B′ (Fig. 1), the Kingsbury Conglomerate is observed only in the ARCO Kenny

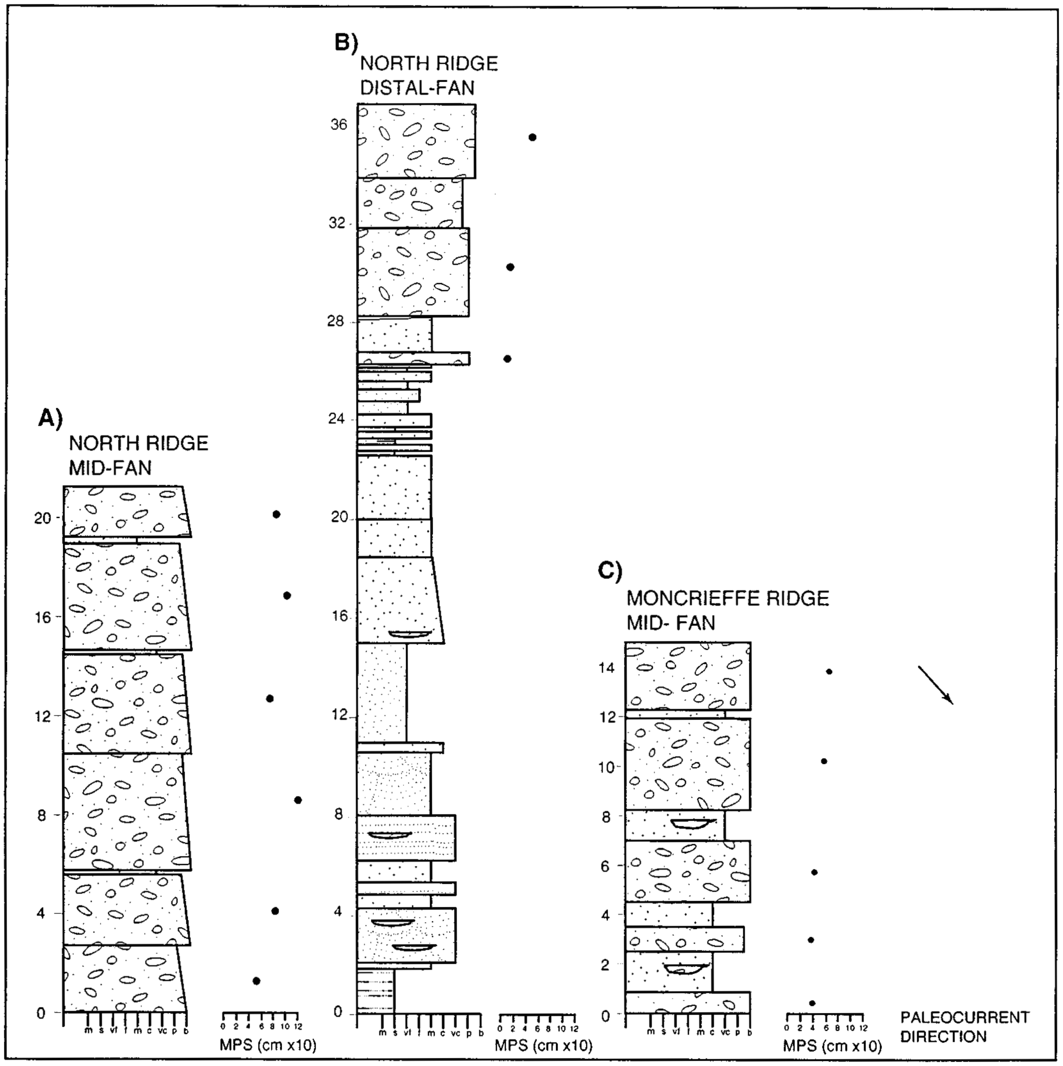

Figure 7. Log of measured stratigraphic sections of the Moncrief Conglomerate with maximum particle size (MPS) and paleocurrent data. (A) Mid-fan deposits at North Ridge. Location 7A in Figure 4B. (B) Distal-fan deposits at North Ridge. Location 7B in Figure 4B. (C) Mid-fan deposits at Moncrieffe Ridge. Location 7C in Figure 4D. See Figure 3 for lithology key and grain-size explanation.

Ranch well logs (well #3 in Figs. 1 and 9). Well cuttings indicate that its clast composition is similar to correlative deposits located elsewhere along the range margin (i.e., predominantly Paleozoic carbonates with a minor Precambrian component). The Kingsbury Conglomerate is exposed along the Clear Creek–Johnson Creek thrust fault to the north along Johnson Creek (Fig. 1). Here, the majority of the conglomerate clasts are Madison Limestone and Bighorn Dolomite (Fig. 5B).

Deformation of Synorogenic Conglomerates. The Moncrief Conglomerate exposed along U.S. Highway 16 is in fault contact with the Clear Creek thrust fault (Fig. 8). Locally, directly beneath the Clear Creek thrust (within 15 m below the thrust fault), a thick sequence of upward-fining beds has been rotated basinward to near vertical orientations. Fault gouge and fractured clasts along bedding planes indicate flexural-slip folding. Directly below this panel of vertically dipping beds is a panel of horizontal strata. Back thrusts and bedding-plane faults have offset conglomerate clasts and locally caused elongation of clasts due to shearing within this lower panel. The lowest exposed and unfaulted proximal fan deposits dip 45°E. Overall, the Moncrief Conglomerate in this area is interpreted to have undergone a minimum of 35° of bed rotation (assuming an initial 10° depositional slope).

Structural Evolution. The two primary fault systems present in the vicinity of North Ridge are the Clear Creek thrust system (CCTF1 and CCTF2 in Fig. 9) and the Buffalo Deep fault (BDF in Fig. 9). The Clear Creek thrust system is interpreted to have directly influenced both the deposition and deformation of the synorogenic deposits. Uplift along cross section B–B′ is 9.57 km; shortening is 9.30 km (26.3%) (Fig. 9D). Two wells, the Arco Kenny Ranch well #1-4 (well #3 in Figs. 1 and 9) and the Buffalo Federal 1-1 well (well #4 in Figs. 1 and 9), were used to determine the relative position of footwall stratigraphy. The Arco Kenny Ranch well (for which a dipmeter survey is available) drilled through 731 m of basement granite in the hanging wall before penetrating the CCTF1 and into 305 m of Kingsbury Conglomerate (Fig. 9D). The well then penetrated an overturned section of Fort Union shales (dipping 70° to the west) before crossing a second fault (CCTF2) at a depth of 1707 m into a normal stratigraphic section dipping 20° to the west (Fig. 9D). The hanging wall of the Clear Creek thrust system places middle and lower Paleozoic carbonate strata on top of the Moncrief Conglomerate (Fig. 8), which is composed of nearly 100% Precambrian clasts.

Cross section B–B′ was retrodeformed in four stages. (1) The initial uplift of the Bighorn Mountains in the North Ridge area began with displacement along the Clear Creek thrust system (CCTF1 and CCTF2 on Fig. 9). This led to the exposure and unroofing of the Mesozoic mudstones and poorly indurated sandstones in the hanging wall. The bulk of eroded hanging-wall

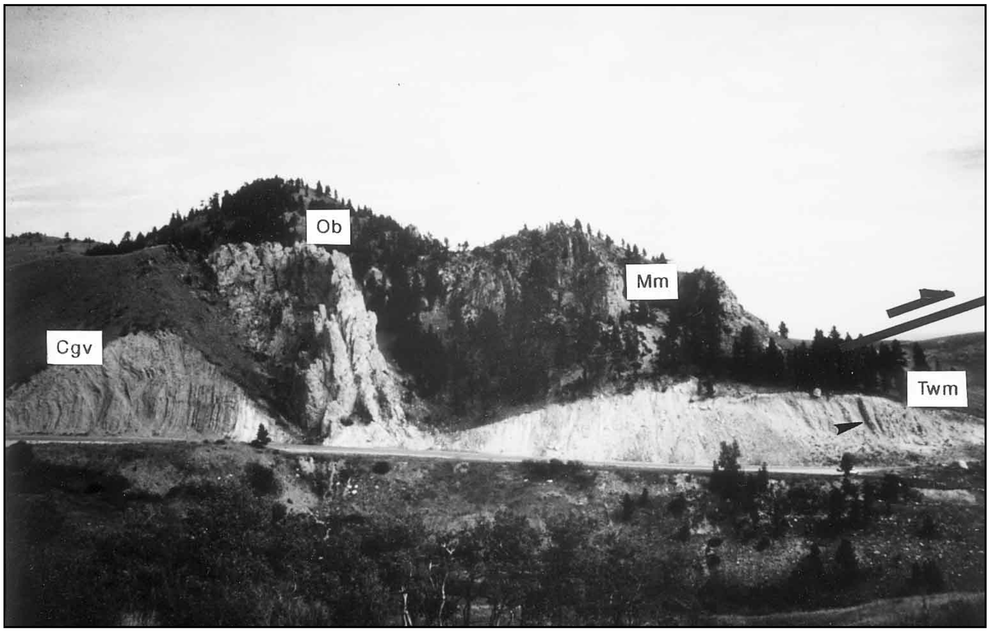

Figure 8. Photograph of the Clear Creek thrust fault along U.S. Highway 16 showing relationship between thrust-faulted basin margin and synorogenic Moncrief Conglomerate. View is toward the north. Solid black line and large arrow indicate thrust fault. Middle and lower Paleozoic strata have been emplaced over Eocene Moncrief Conglomerate. Note the steeply dipping Moncrief Conglomerate (Twm) in footwall (small arrow). Vertically dipping hanging-wall units include: Cgv—Cambrian Gros Ventre Formation, Ob—Ordovician Bighorn Dolomite, and Mm—Mississippian Madison Limestone.

sediment was transported out of the most proximal part of the basin, resulting in the deposition of the Lebo Shale Member of the Paleocene Fort Union Formation. At this stage, uplift was 3.96 km with 2.05 km of shortening (6.0%) (Fig. 9A). During this initial stage of deformation, the footwall growth syncline was an open fold hinged at the tip of CCTF2 (Fig. 9A). (2) Continued displacement along the CCTF1 exposed the more durable middle and lower Paleozoic units in the hanging wall. Unroofing of these units led to the deposition of the Kingsbury Conglomerate observed in the Kenny Ranch well logs. Uplift at the onset of the Kingsbury Conglomerate deposition was 6.01 km, and shortening was 5.86 km (16.6%) (Fig. 9B). During this stage of deformation, rotation of the steeper, western limb of the growth syncline was caused by coeval displacement on the CCTF1 and the CCTF2 as CCTF2 began to propagate through the fold hinge (Fig. 9B). (3) After deposition of approximately 300 m of the Kingsbury Conglomerate, displacement was transferred to a splay of the CCTF1 (FS1 in Fig. 9C). Displacement along this splay resulted in the exposure of the Precambrian basement rocks that were the source terrane for the Moncrief Conglomerate. Uplift at the onset of the Moncrief Conglomerate deposition was 7.44 km, and shortening was 6.65 km (18.8%) (Fig. 9C). During this stage of deformation, the Moncrief Conglomerate was deposited along the hinge of the footwall growth syncline above the Kingsbury Conglomerate (Fig. 9, C and D). The Moncrief Conglomerate appears to have undergone 35° of eastward syndepositional rotation as it was incorporated into the growing footwall syncline. (4) After deposition of the Moncrief Conglomerate, reactivation of the CCTF1 truncated the western limb of the footwall syncline coeval with propagation of CCTF2 through the hinge of the syncline. This last stage of deformation juxtaposed the lower Paleozoic strata over the Eocene synorogenic deposits, as observed along the U.S. Highway 16 road cut (Figs. 8 and 9D). Note that, unlike at Kingsbury Ridge, the Buffalo Deep fault does not appear to directly influence synorogenic deposition, despite its most likely displacement during the Kingsbury Conglomerate deposition.

Mowry Basin

Stratigraphy. Synorogenic conglomerates in the Mowry basin include the Paleocene Fort Union conglomerate and the Kingsbury Conglomerate (Fig. 1). The Fort Union conglomerate is predominantly a clast-supported, channelized conglomerate interbedded with fine sandstone-siltstone paleosols (Fig. 10). In surface exposures, the Fort Union conglomerate is 430 m thick, and maximum particle size data from the top 160 m show a progressive upward-fining sequence, from around 20 cm at the base of the measured section to about 9 cm at the top (Fig. 10). Occasional matrix-supported conglomerate units, interpreted as debris-flow deposits, have a maximum particle size close to 50 cm. Many of the conglomeratic intervals exhibit pebble imbrication showing two directions of paleoflow alternating between nearly due south and northeast (Fig. 4C). The Kingsbury Conglomerate overlies the Fort Union conglomerate in the Mowry basin and contains mainly clast-supported, channelized conglomerates. The Kingsbury Conglomerate has more trough cross-stratification than the Fort Union conglomerate, as well as a greater abundance of interbedded sandstone and mudstone (Figs. 3B and 10). Maximum particle size data show an upward-coarsening package from 10 cm at the base of our measured section to near 20 cm at the top (Fig. 3B). Paleocurrent measurements from cross-stratification and pebble imbrication show sediment transport directions to the east-southeast (Fig. 4C).

Clast Composition. The Fort Union conglomerate consists of nearly 90% Mississippian Madison Limestone and Ordovician Bighorn Dolomite clasts and 10% Cambrian Gros Ventre Formation and Cambrian Flathead Sandstone clasts (Fig. 5C). There is little change in clast composition upsection (Hoy, unpub. data). The Kingsbury Conglomerate in the Mowry basin contains 75% Mississippian Madison Limestone and Ordovician Bighorn Dolomite clasts (50% and 25%, respectively), 25% Cambrian Flathead and Gros Ventre clasts, and <1% Precambrian basement clasts (Fig. 5C).

Deformation of Synorogenic Conglomerates. The synorogenic conglomerates in the Mowry basin have undergone significant progressive bed rotation. In the Fort Union conglomerate, the basal strata are dipping as much as 40°E, whereas strata at the top of the section dip about 20°E. An angular unconformity of 10° exists between the Fort Union conglomerate and the Kingsbury Conglomerate. Intraformational rotation in the Kingsbury Conglomerate is less evident than in the underlying Fort Union conglomerate. The basal Kingsbury strata locally dip as much as 20°E, but the predominant bedding attitudes at the base of the Kingsbury Conglomerate are 10°E.

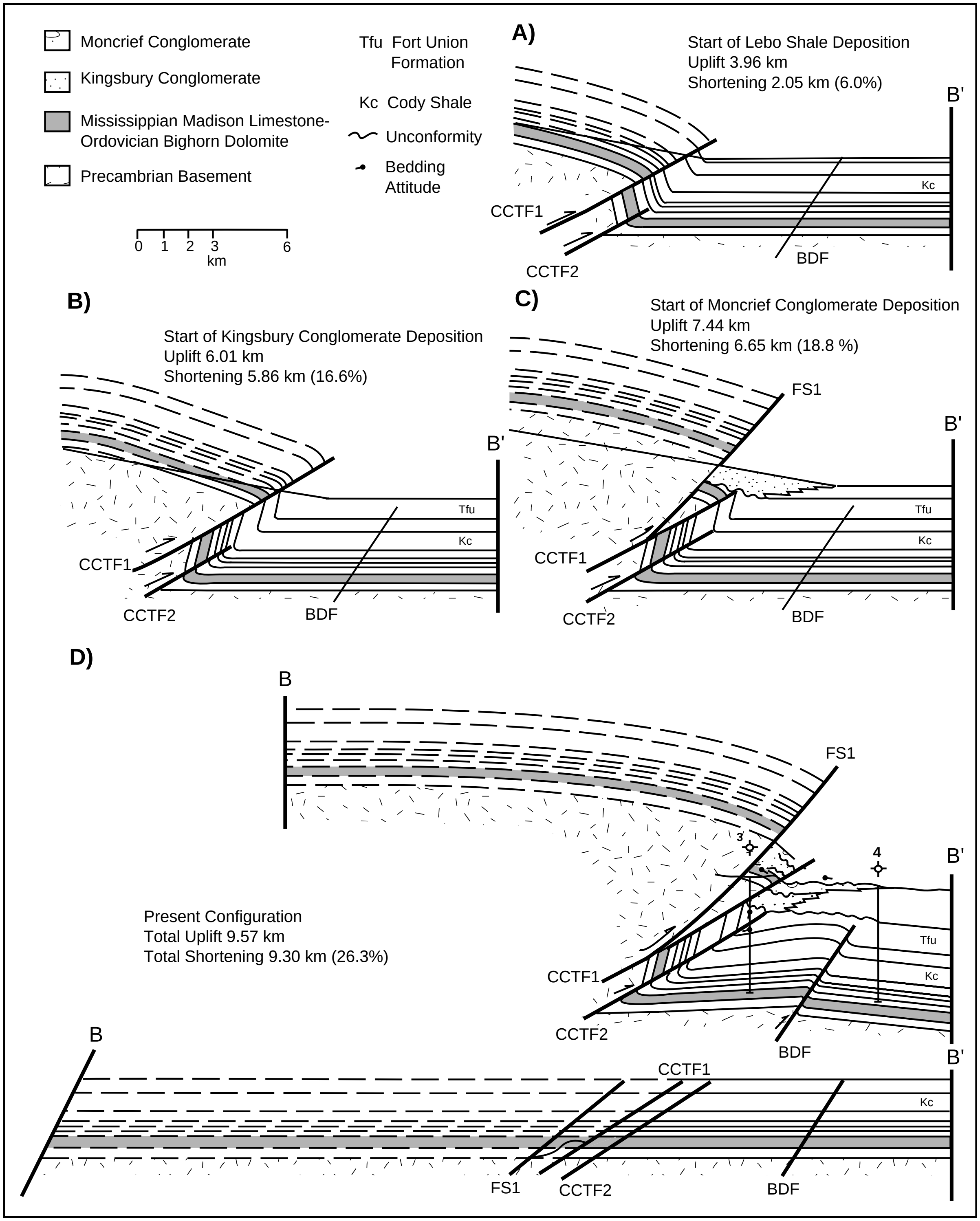

Figure 9. Sequential restoration of cross section B–B′ at North Ridge (see Fig. 1 for location of cross section). Amount of uplift and shortening is shown for each stage of retrodeformation. (A) Initial displacement along the Clear Creek thrust system (CCTF1 and CCTF2) and beginning of Lebo Shale deposition in the Powder River basin. (B) Continued displacement along CCTF1 and start of Kingsbury Conglomerate deposition. (C) Displacement transferred to splay FS1 of the CCTF1 marks onset of Moncrief Conglomerate deposition. (D) Reactivation of CCTF1 to present-day structural configuration. Petroleum well logs used for construction: 3—Arco Kenny Ranch #1-4 well; 4—Buffalo Federal 1-1 well. BDF—Buffalo Deep fault.

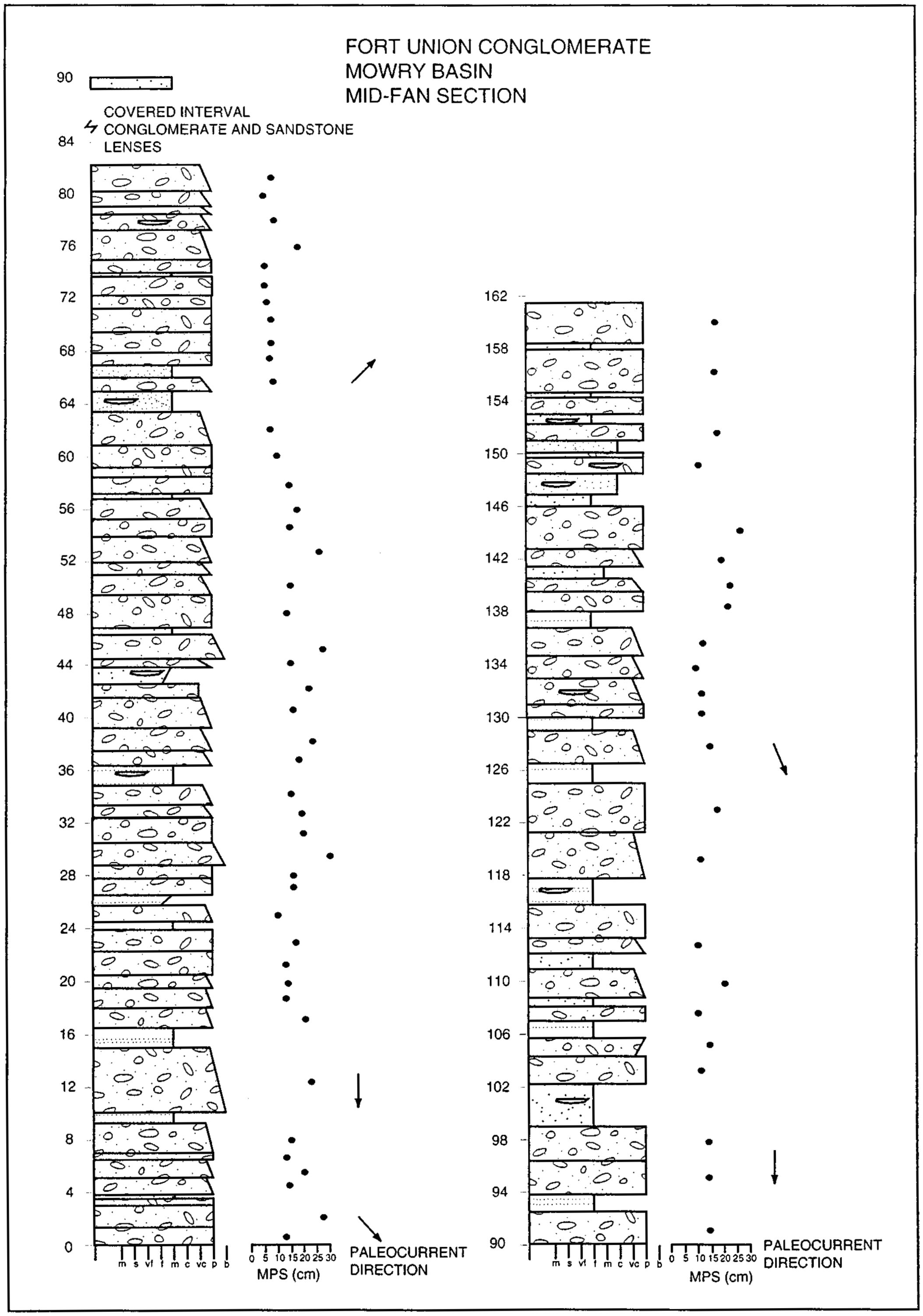

Figure 10. Log of measured stratigraphic section of mid-fan deposits of the Fort Union conglomerate in the Mowry basin with maximum particle size (MPS) and paleocurrent data. Location 10 in Figure 4C. See Figure 3 for explanation of lithology key and grain-size explanation.

Structural Evolution. Deposition of the conglomerates in the Mowry basin resulted from basinward rotation between the Mowry basin thrust fault and the Johnson Creek thrust fault (MBTF and JCTF in Fig. 11). As at North Ridge (Fig. 9), the Buffalo Deep fault is located farther east in the Powder River basin, well away from the synorogenic deposits, and as a result did not influence conglomerate deposition in the Mowry basin. Uplift along cross section C–C′ is 8.14 km, and shortening is 5.1 km (14.2%) (Fig. 11D).

Cross section C–C′ was retrodeformed in four stages. (1) Initial movement along the Mowry basin thrust resulted in deposition of the Lebo Shale, which was derived from the erosion of Mesozoic and upper Paleozoic units. During initial growth syncline development, the syncline was hinged at the

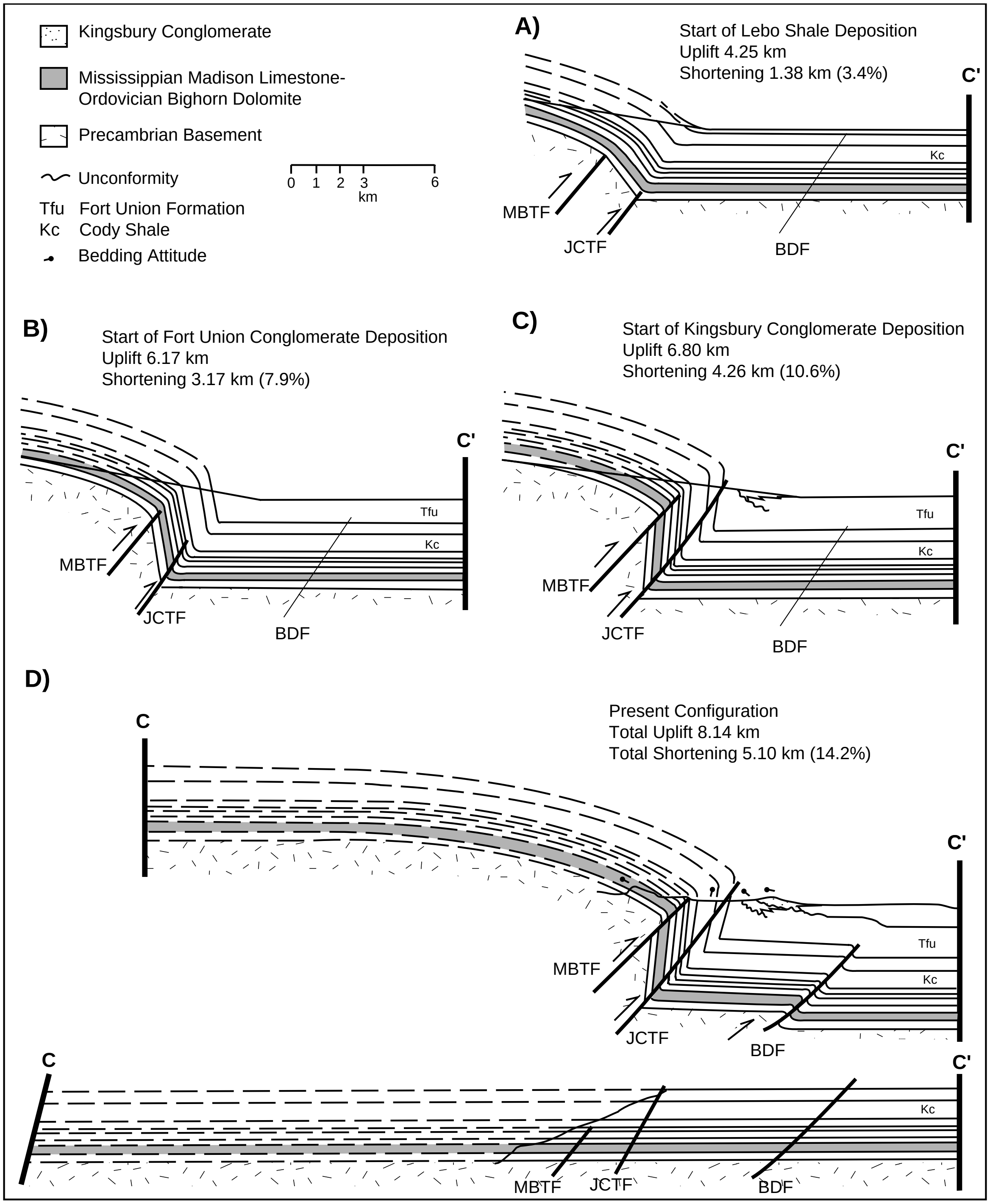

Figure 11. Sequential restoration of cross section C–C′ at the Mowry basin (see Fig. 1 for location of cross section). Amount of uplift and shortening is shown for each stage of retrodeformation. (A) Initial displacement along the Mowry Basin thrust fault (MBTF) and start of Lebo Shale deposition in the Powder River basin. (B) Farther displacement along MBTF and the Johnson Creek thrust fault (JCTF) and onset of Fort Union conglomerate deposition. (C) Continued displacement along the MBTF and the JCTF and onset of Kingsbury Conglomerate deposition. (D) Displacement along the MBTF and the JCTF to present structural configuration. BDF—Buffalo Deep Fault.

tip of the JCTF (Fig. 11A). Uplift at this stage was 4.25 km with 1.38 km of shortening (3.4%) (Fig. 11A). Much of the sediment derived from the uplifted source terrane bypassed the proximal region and was deposited farther out in the basin. (2) Continued displacement on the Mowry basin thrust fault exposed the Mississippian Madison Limestone and Ordovician Bighorn Dolomite and resulted in the deposition of the Fort Union conglomerate (Fig. 11B). Uplift at this phase was 6.17 km, and shortening was 3.17 km (7.9%) (Fig. 11B). During this stage the Johnson Creek thrust fault began to propagate through the hinge of the fold. Continued basinward rotation of the strata between the Mowry basin thrust fault and the Johnson Creek thrust fault produced the progressive unconformities found within the Fort Union conglomerate. (3) Additional displacement and uplift along the Mowry basin thrust fault allowed for the increased dissection of the hanging wall (Fig. 11C). This accounts for the increased contribution of Cambrian clasts within the Kingsbury Conglomerate. Uplift at the onset of the Kingsbury Conglomerate deposition was 6.80 km, and shortening was 4.26 km (10.6%) (Fig. 11C). During this stage the Johnson Creek thrust fault propagated through the entire hinge of the growth syncline. (4) During the latest stages of displacement, block rotation between the Mowry basin thrust fault and the Johnson Creek thrust fault caused the western limb of the growth syncline to become slightly overturned (Fig. 11D). As much as 10° of syndepositional rotation occurred within the Kingsbury Conglomerate during this stage.

Piney Creek Thrust Block

Stratigraphy. The northernmost synorogenic conglomerates are exposed adjacent to the Piney Creek thrust block, a large basement-involved thrust block flanked on the north and south by northeast-southwest–striking tear faults (Fig. 1). Two conglomerates, the Kingsbury Conglomerate and the Moncrief Conglomerate, are exposed basinward of the Piney Creek thrust (Fig. 1). The Kingsbury Conglomerate is exposed at the base of Moncrieffe Ridge and in one location farther south along the Piney Creek thrust block (Fig. 1). Maximum particle size data from the Kingsbury Conglomerate average between 15 and 30 cm (Fig. 4D). The best exposures of the Moncrief Conglomerate occur on Moncrieffe Ridge (Fig. 1). This alluvial fan deposit (Sharp, 1948; Obernyer, 1979) is lithologically very similar to that of North Ridge (Fig. 1); clast-supported, boulder conglomerate facies in proximal fan deposits grade laterally into finer mid-fan (Fig. 7C) and distal fan deposits. Less-extensive deposits of Moncrief Conglomerate occur along the length of the Piney Creek thrust block (Fig. 1). Maximum particle size data from the Moncrief Conglomerate range from about 9 cm in the distal sections to as much as 200 cm in the proximal deposits (Fig. 4D). The Kingsbury Conglomerate in this area has paleocurrent indicators that document north-northeastward and southeastward paleoflow, whereas paleocurrent indicators in the Moncrief Conglomerate display southeastward paleoflow (Fig. 4D).

Clast Composition. Conglomerate clast composition is well defined on Moncrieffe Ridge. A velocity test hole was drilled on Moncrieffe Ridge (well #2 in Figs. 1 and 12) in association with the Granite Ridge well (well #1 in Figs. 1 and 12) drilled through the hanging wall of the thrust block. The test hole sample logs (i.e., mud logs) did not show an abrupt compositional change from Kingsbury Conglomerate (predominantly Paleozoic clasts) to Moncrief Conglomerate (nearly 100% Precambrian basement clasts), but instead showed a gradual change from 100% sedimentary clasts of Mississippian Madison Limestone, Ordovician Bighorn Dolomite, and Cambrian Gros Ventre Formation at a depth of 533 m, to 100% basement clasts of granite and gneiss at a depth of 232 m. Sample logs indicate that the contact between the Kingsbury and Moncrief Members was arbitrarily placed at the first appearance of sedimentary clasts in the drill cuttings. Outcrops of the Kingsbury Conglomerate, adjacent to the Piney Creek thrust (labeled A–D in Figs. 4D and 5D), also have clast compositions that document a gradual transition from primarily sedimentary clasts to crystalline Precambrian clasts.

Deformation of Synorogenic Conglomerates. The footwall synorogenic conglomerates of the Piney Creek thrust block show little deformation. The Kingsbury Conglomerate shows a maximum of 20° of rotation (assuming an original 10° depositional slope), but deformed conglomerate clasts were not found.

Structural Evolution. Uplift along the Piney Creek thrust block was controlled by the two imbricate faults of the Piney Creek thrust fault system (PCTF1 and PCTF2 in Fig. 12) that dip approximately 25°W. The Buffalo Deep fault is located under the distal deposits at Moncrieffe Ridge (Figs. 1 and 12D). However, the fault does not appear to have influenced deposition or deformation within these synorogenic deposits. Data from the Granite Ridge well help determine the location of the Piney Creek thrust fault and footwall strata (well #1 in Fig. 12D). This well was spudded in Precambrian granite and drilled through 753 m of granite before it penetrated a thrust fault (PCTF1). After crossing the thrust fault, the well entered an overturned section of Upper Cretaceous strata, then crossed a second fault (PCTF2) into nearly horizontal strata of the same age (Fig. 12D). Uplift along cross section D–D′ is 9.90 km, and shortening is 8.89 km (21.9%) (Fig. 12D).

Cross section D–D′ was retrodeformed in four stages. (1) Initial displacement and uplift along the Piney Creek thrust fault (PCTF1) initiated unroofing of the Mesozoic and upper Paleozoic source section and deposition of the Lebo Shale in the Powder River basin (Fig. 12A). Uplift at this stage was 5.1 km, and shortening was 2.61 km (6.6%) (Fig. 12A). During this early stage of fold development, the growth syncline was hinged at the top of PCTF2. (2) Continued thrust displacement and erosion exposed the middle and lower Paleozoic carbonate rocks in the hanging wall and generated the Kingsbury Conglomerate (Fig. 12B). The fine-grained members of the Fort Union Formation were rotated into the steeper limb of the growth syncline during this stage. This rotation produced the unconformity between the Fort Union Formation and the Kingsbury Conglomerate. During this stage the PCTF2 propagated partially through the hinge of the growth syncline. Uplift at the onset of Kingsbury Conglomerate deposition was 6.49 km, and shortening was 6.15 km (15.5%) (Fig. 12B). (3) Additional displacement along the Piney Creek thrust fault exposed Precambrian basement rocks, resulting in the deposition of the Moncrief Conglomerate (Fig. 12C). Uplift at this stage was 8.99 km, and shortening was 7.95 km (19.2%) (Fig. 12C). (4) In the final stage of deformation, the Piney Creek thrust block was thrust over the conglomerates at Moncrieffe Ridge, resulting in the configuration observed today (Fig. 12D). The change in conglomerate clast composition (Fig. 5D) suggests that the structural evolution from stage 2 through stage 4 in Figure 12 was a gradual transition rather than a series of discrete events, as indicated by angular unconformities between the Kingsbury Conglomerate and the Moncrief Conglomerate in other areas along the range margin.

GENERAL IMPLICATIONS

Structural Development of Growth Synclines

Our analysis of the configuration of the east-central Bighorn Mountains identified three structural stages of footwall growth syncline development associated with fault-related folding.

Stage I. The structural configuration of two areas, Kingsbury Ridge (A–A′ in Figs. 1 and 6) and the Mowry Basin (C–C′ in Figs. 1 and 11), is interpreted to be the product of deformation during the earliest part of fault-related fold development. Our cross sections (Figs. 6 and 11) show that the structural configuration of the range margin in both areas was controlled by imbricate basement-involved blind thrusts. The surface expression of the blind thrusts is an anticline-syncline pair (Fig. 13A). Paleozoic strata in the shared fold limb dip between 20° and 65° toward the Powder River basin (Fig. 14). Eastward, the Mesozoic strata show a steepening of dips upsection in the shared fold limb and locally become overturned (Fig. 14). Coarse synorogenic sediments were deposited in the developing growth syncline and in places onlapped the eroded, steeply dipping Mesozoic strata (Fig. 14). The onlap relationship indicates that significant limb rotation and erosion occurred prior to deposition of the conglomerates.

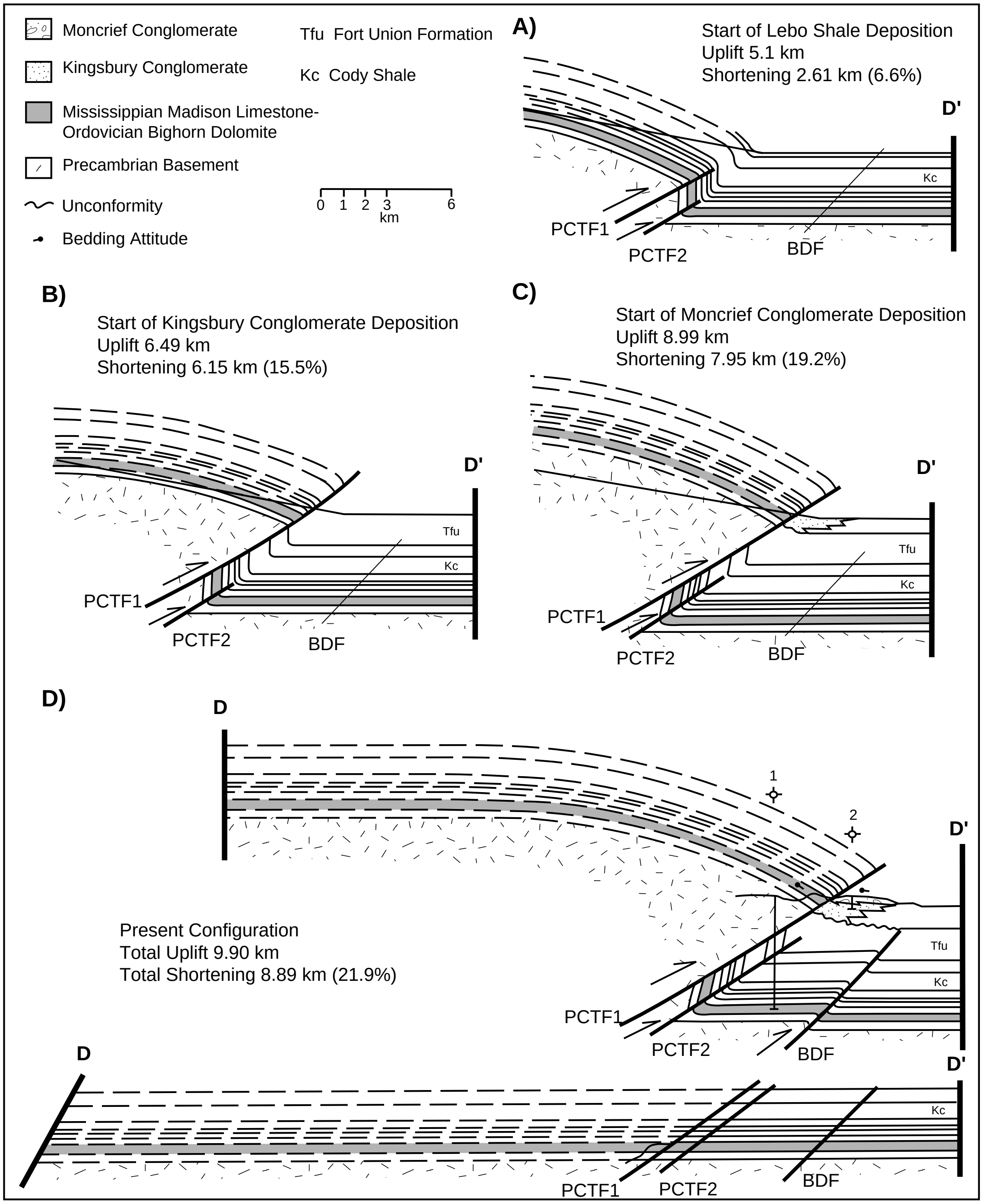

Figure 12. Sequential restoration of cross section D–D′ at Moncrieffe Ridge (see Fig. 1 for location of cross section). Amount of uplift and shortening is shown for each stage of retrodeformation. (A) Initial displacement along the Piney Creek thrust system (PCTF1 and PCTF2) and beginning of Lebo Shale deposition in the Powder River basin. (B) Further displacement along PCTF1 and start of Kingsbury Conglomerate deposition. (C) Continued displacement along PCTF1 and onset of Moncrief Conglomerate deposition. (D) Displacement along PCTF1 and PCTF2 to present structural configuration. Petroleum well logs used for construction: 1—Granite Ridge 1-2-9D well, 2—Granite Ridge velocity test hole. BDF—Buffalo Deep fault.

Two depositional episodes occurred along the western margin of the Powder River basin during stage 1 deformation. First, deposition of the Lebo Shale occurred during the initial displacement on the range-bounding faults. Our cross sections show that at the end of Lebo Shale deposition, there was an average of 6.46 km of uplift and 4.60 km of shortening along the eastern Bighorn Mountains (Table 1). During the second depositional episode, the Fort Union conglomerate and the Kingsbury Conglomerate were deposited (Fig. 13A). Fold limb rotation due to fault propagation in-

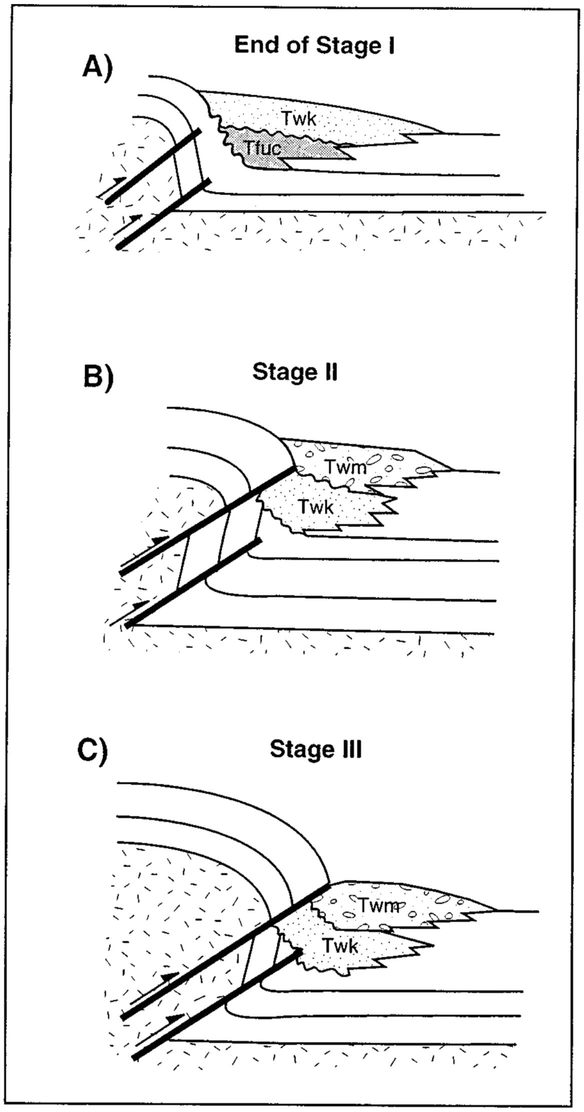

Figure 13. Schematic cross sections illustrating various stages of footwall growth syncline development along the east-central flank of the Bighorn Mountains. (A) The end of stage I deformation as seen at the Mowry basin represents the early development of the growth syncline. Note the anticline-syncline pair above the blind thrust faults and the deposition of synorogenic sediments along the hinge of the syncline. Key for figure: jackstraw pattern represents Precambrian crystalline basement rocks; beds without patterns represent Paleozoic and Mesozoic rocks; Tfuc—Fort Union conglomerate; Twk—Kingsbury Conglomerate; Twm—Moncrief Conglomerate. (B) Stage II represents the intermediate stage of growth syncline evolution as documented at Johnson Creek. Note that the thrust system partially truncated the growth syncline. Note rotation of Paleozoic and Mesozoic strata in the shared fold limb to a steeper dip (relative to stage I). Fold limb rotation resulted in development of progressive unconformities (not shown) in synorogenic conglomerate within the growth syncline. (C) Stage III deformation as represented by the structural configuration seen along the Clear Creek thrust system at North Ridge. Note that the thrust system has completely truncated the footwall growth syncline and overrode the entire synorogenic package.

fluenced coarse-grained synorogenic sedimentation in two ways. First, alluvial-fan deposits underwent a gradual eastward rotation that resulted, over time, in a progressive fanning and decrease of dips upsection (Fig. 14). The most proximal fan deposits were incorporated into the shared fold limb and were uplifted, eroded, and redeposited basinward. Second, the continued uplift of the proximal part of the growth syncline caused a basinward progradation of subsequent alluvial-fan deposits (Fig. 13A). The Kingsbury Conglomerate is the most widespread of all the synorogenic conglomerates in the study area and was deposited along the entire east-central margin of the Bighorn Mountains. Our cross sections and the distribution of the Kingsbury Conglomerate indicate that the deformation represented by stage I occurred throughout the study area. Stage I is interpreted as the earliest stage of fault-related fold development. After Kingsbury Conglomerate deposition, there was an average of 8.17 km of uplift and 6.36 km of shortening (Table 1).

Stage II. The exposures on the north side of Johnson Creek (Fig. 1) are representative of stage II (Fig. 13B). The Moncrief Conglomerate was deposited during stage II, and overlies the Kingsbury Conglomerate with as much as 95° of angular discordance (Fig. 15). The lower portion of the Moncrief Conglomerate has been rotated basinward in the developing growth syncline in a manner similar to that of the Kingsbury Conglomerate during earlier stages of deformation (Fig. 9, C and D). At Johnson Creek, the Johnson Creek thrust has overridden the Kingsbury Conglomerate, which is overturned in the footwall (Fig. 15). The overlying Moncrief Conglomerate, however, is undeformed and dips approximately 10°E (Fig. 15). In this case, the advancing thrust fault partly truncated the footwall growth syncline, but did not override the entire synorogenic package, as seen in stage III at North Ridge (Fig. 8).

Stage III. The final stages of fault-related fold development are represented by the present configuration of the Clear Creek thrust fault (B–B′ in Figs. 1 and 9D) and the Piney Creek thrust block (D–D′ in Figs. 1 and 12D). Surface expressions of stage III are thrust faults that place middle and lower Paleozoic strata in fault contact with the synorogenic Moncrief Conglomerate of the Wasatch Formation (Fig. 13C). The Paleozoic strata are the leading edge of a large hanging-wall anticline and range in dip from 30°E in the Cambrian Flathead Sandstone at the core of the fold, to as much as 50°W overturned in the Mississippian Madison Limestone at the edge of the advancing limb. Hanging-wall Mesozoic strata had been removed by prior unroofing associated with earlier stages of deformation.

During the final stages of fault-related folding, the initially blind thrusts propagated into the near-surface conglomerate deposits, truncated the footwall syncline, and overrode the entire synorogenic package (Fig. 13C). During fault truncation of the growth syncline, adjacent footwall synorogenic conglomerate deposits were deformed. Along U.S. Highway 16, for example, beds of the Moncrief Conglomerate have been rotated to near vertical (Fig. 8), and boulder-sized clasts have been deformed along numerous back thrusts and flexural slip surfaces (Hoy, 1996). Cross sections through the Clear Creek thrust fault and Piney Creek thrust block indicate that these areas, characteristic of stage III, have undergone an average of 9.74 km of uplift and 9.10 km of shortening (Table 1).

Implications for Fault-Related Fold Models

The deposition and deformation of the synorogenic deposits along the east-central Bighorn Mountains are a direct result of the formation of folds associated with basement-involved faults. The fold styles shown by our cross sections are similar to “thick-skinned” folding styles associated with basement faults that have propagated upsection into sedimentary cover rocks (Brown, 1983, 1988; DeCelles et al., 1991; McConnell and Wilson, 1993; Schmidt et al., 1993; Stone, 1993). The folds along the east-central Bighorn

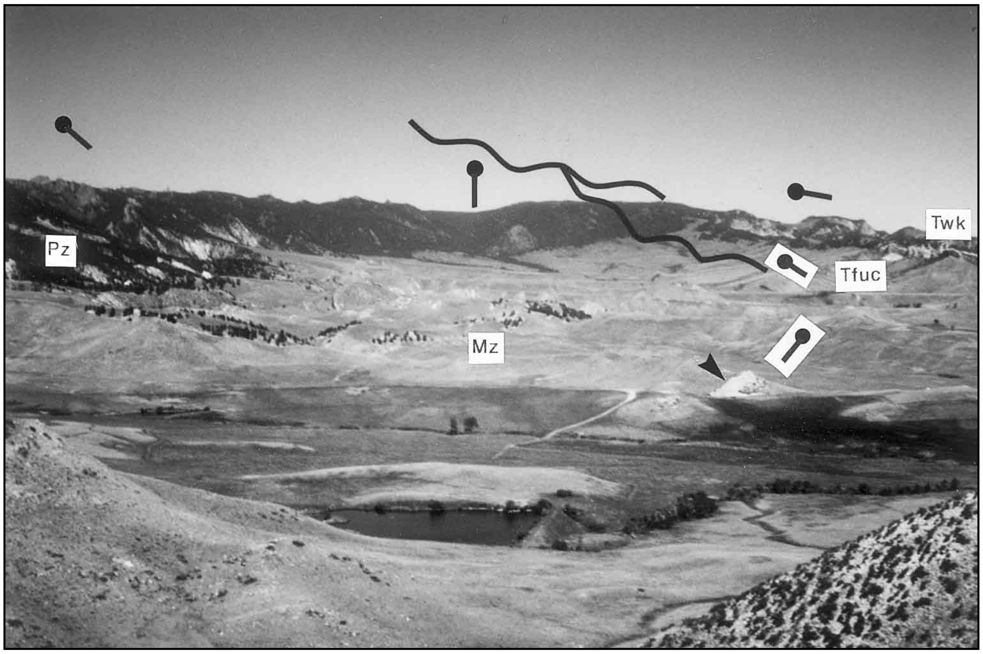

Figure 14. Shared limb of an anticline-syncline pair characteristic of stage I deformation in the Mowry basin. View is to the north. Tadpole symbols indicate dips, and sinusoidal lines indicate unconformities. Paleozoic strata (Pz) in the shared fold limb dip approximately 50°E (to right) toward the Powder River basin. Eastward, Mesozoic strata (Mz) show a steepening of dips upsection and eventually become overturned in the shared fold limb. Arrow points to a well-exposed overturned Cretaceous outcrop dipping to the west (left). Shallow-dipping synorogenic Tertiary conglomerates, the Fort Union conglomerate (Tfuc) and the Kingsbury Conglomerate (Twk) were deposited in the hinge of the developing growth syncline. Note that the synorogenic deposits onlap the eroded, steeply dipping Mesozoic strata with an angular unconformity. This onlap relationship indicates that significant limb rotation and erosion occurred prior to deposition of the conglomerates. Continued limb rotation during conglomerate deposition produced an additional angular unconformity that separates Tfuc and Twk (note the change in dip between the two units). Compare this figure with schematic diagrams shown in Figure 13 (A and B).

Mountains are different than those described by "thin-skinned" classic fault-propagation fold models (Suppe, 1983; Mitra, 1990). In our study area, for example, angular and progressive unconformities in the proximal limb of the footwall growth syncline are evidence that the forelimb was progressively rotated to a steeper dip. In the classic geometric models of fault-propagation folding, limb dips are attained instantaneously and do not change after fold growth begins (see Fischer et al., 1992, for discussion). These results support a growing number of studies suggesting that limb rotation is an important component in the growth of some fault-related folds (Anadon et al., 1986; DeCelles et al., 1991; Holl and Anastasio, 1993; Poblet and Hardy, 1995; Vergés et al., 1996; Zapata and Allmendinger, 1996).

McConnell (1994) proposed a basement-involved model in which the thrust fault propagates through the forelimb of the fold. In his model, the footwall syncline is hinged where the fault intersects the basement–sedimentary cover contact. Continued fault propagation rotates the forelimb strata in both the hanging wall and footwall. McConnell's model describes many of the structural features documented in the eastern Bighorn Mountains, but does not include the imbricate fault pair observed in the study area. Block rotation between imbricate fault pairs interpreted for the Bighorn Mountains is similar to that discussed by Kellogg et al. (1995) for Laramide uplifts in Montana.

Implications for Laramide Uplift and Unroofing of the Bighorn Mountains

Estimates of the initiation of Laramide uplift of the Bighorn Mountains have ranged from Late Cretaceous (Gries et al., 1992; Hansley and Brown, 1993), to late Paleocene (Sharp, 1948; Hose, 1955; Mapel, 1959; Merin and Lindholm, 1986). Isopach maps of the members of the Fort Union Formation indicate that subsidence in the Powder River basin began in the early to middle Paleocene, as indicated by thickening of the Lebo Shale member from about 8 m in the eastern part of the basin to 915 m adjacent to the east-central Bighorn Mountains (Curry, 1971; Flores and Ethridge, 1985, Fig. 4). The Lebo Shale has been interpreted as an extensive fluvial-lacustrine facies that formed along the western margin of the Powder River basin (Lake Lebo) (Flores and Ethridge, 1985; Flores, 1986; Ayers, 1986). Previous studies concluded that Lake Lebo was filled entirely by deltas prograding from the ancestral Black Hills, Casper Arch, and Laramie Mountains. The lack of coarse detritus in the lower Fort Union deposits was interpreted as evidence that the adjacent Bighorn Mountains provided little sediment to the forming basin (Curry, 1971; Tewalt et al., 1983; Flores and Ethridge, 1985; Ayers, 1986; Flores, 1986). These studies suggested that the first indication of uplift and erosion of the Bighorn Mountains was contained in the sandstones of the Tongue River Member and the Fort Union conglomerate (Fig. 2), and that major uplift began during the Eocene with deposition of the Kingsbury and Moncrief conglomerates.

In contrast to the traditional interpretation outlined above, results of this study indicate that, by the onset of middle Paleocene Lebo Shale deposition, an average of 3.8 km of uplift and 4.50% of shortening had already occurred (Figs. 6, 9, 11, and 12). The subsidence indicated by isopach data of the Lebo Shale (Curry, 1971; Ayers, 1986) had to be accompanied by erosion of approximately 2 km of mainly Mesozoic mudstone from the hanging

TABLE 1. RESULTS OF UPLIFT AND SHORTENING CALCULATIONS

Depositional stage*	Map location	Cross section	Uplift (km)	Shortening (km)	Shortening (%)
Onset Twk	Kingsbury Ridge	A–A′	6.55	2.13	5.8
	North Ridge	B–B′	6.01	5.86	16.6
	Mowry basin	C–C′	6.80	4.26	10.6
	Piney Creek thrust block	D–D′	6.49	6.15	15.5
End Twk	Kingsbury Ridge	A–A′	8.10	5.73	15.5
	North Ridge	B–B′	7.44	6.65	18.8
	Mowry basin	C–C′	8.14	5.10	14.2
	Piney Creek thrust block	D–D′	8.99	7.95	19.2
End Twm	North Ridge	B–B′	9.57	9.30	26.3
	Piney Creek thrust block	D–D′	9.90	8.89	21.9

*Twk—Kingsbury Conglomerate, Twm—Moncrief Conglomerate.

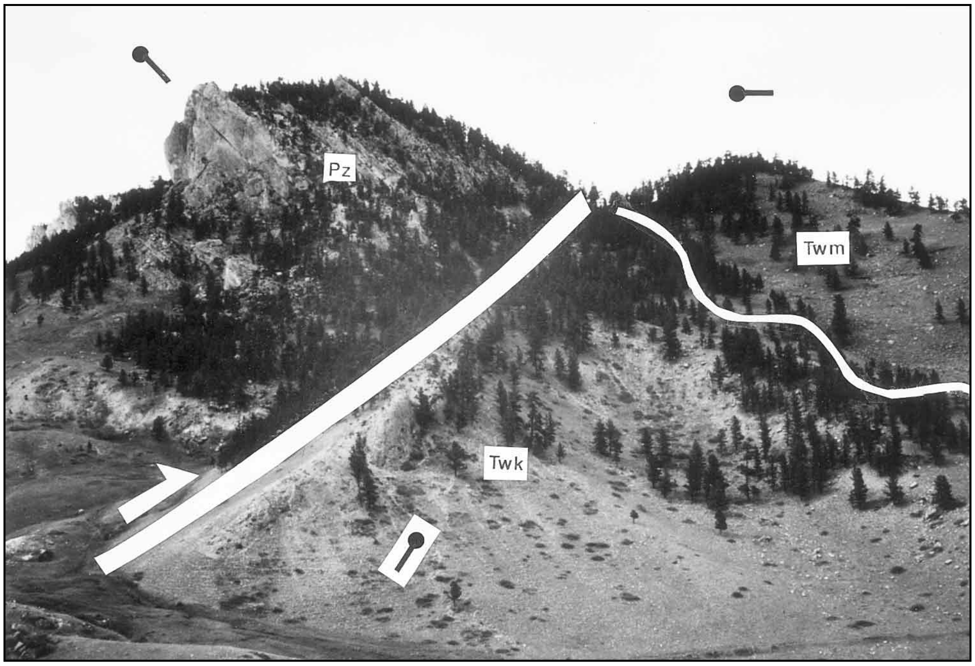

Figure 15. Photograph of structural relationship exposed on Johnson Creek that is characteristic of stage II deformation. View is looking north at the Johnson Creek thrust (thick solid white line). Tadpole symbols indicate dip directions, thin sinusoidal line indicates angular unconformity, and arrow indicates displacement direction on thrust fault. In the hanging wall, Mississippian Madison Limestone (Pz) is dipping 70°E. In the footwall, overturned Eocene Kingsbury Conglomerate (Twk) is dipping 60°W. The Moncrief Conglomerate (Twm), which unconformably overlies the Kingsbury Conglomerate, dips approximately 10°E. The lack of deformation and bed rotation in the Moncrief Conglomerate indicates that it has not been overridden by the Johnson Creek thrust (cf. Fig. 13B). In this example, the thrust fault has partially truncated the growth syncline but did not override all of the synorogenic conglomerates in the footwall.

wall of the Bighorn thrust system. The Permian through Cretaceous hanging-wall stratigraphic-source section is composed predominantly of mudstone and subordinate poorly indurated sandstone (Fig. 2) that is incapable of generating coarse detritus. Prior to the accumulation of the Kingsbury Conglomerate, roughly 2.8 km of stratigraphic-source section had been eroded from the eastern Bighorn Mountains. Stripping of these nonresistant rocks from the Bighorn Mountains must be accounted for by deposition within the Powder River basin, because it is unlikely that the sediments generated by erosion of the entire Mesozoic section bypassed the local depocenter within the growing basin (i.e., Lake Lebo). Our results suggest that the 914 m of Lebo Shale adjacent to the thrusted east-central segment of the Bighorn Range is at least partly the product of unroofing of the Mesozoic strata in the nearby hanging-wall section (Fig. 16A). The lack of coarse detritus in the thick sections of the Lebo Shale along the western basin margin is in fact what should be expected from the uplift of the Bighorn source terrane. In addition, the presence of Lake Lebo adjacent to the east-central Bighorn Mountains can be used to infer that there was enough local relief to result in ponding of water. Our interpretation does not preclude the possibility of additional sediment contribution from other nearby uplifts into Lake Lebo (Flores and Ethridge, 1985; Ayers, 1986). By the end of the Paleocene, Lake Lebo had been filled and a regional fluvial system had developed (Tongue River deposits). During this time, the alluvial-fan system that deposited the Fort Union conglomerate found in the Mowry basin was active. The Fort Union conglomerate is found only in the Mowry basin, indicating that the fan was of local significance (Fig. 16A). The initiation of Kingsbury Conglomerate deposition marks the exposure of durable middle and lower Paleozoic strata in the hanging wall along the entire east-central range margin (Fig. 16B). The onsets of the later stages of fault-related folding were marked by the exposure of Precambrian rocks in the hanging walls of Clear Creek and Piney Creek thrust faults, and deposition of the Moncrief Conglomerate (Fig. 16C).

The calculated 8 to 10 km of maximum uplift for the east-central Bighorn Mountains is in general agreement with estimates of 5 to 10 km of uplift associated with other Laramide uplifts (see Dickinson et al., 1988, for review). Assuming that the Bighorn Mountains were at sea level at the end of the Cretaceous, our cross sections indicate about 9.5 km of total rock uplift, about 5.5 km of exhumation, and about 4 km of net surface uplift. Assuming a 20 m.y. active tectonic period (middle Paleocene to middle Eocene), bulk (rock) uplift of the Bighorn Mountains was on the order of approximately 50 cm/1000 yr.

CONCLUSIONS

(1) The earliest stage of growth syncline formation (stage I) along the eastern Bighorn Mountains was characterized by development of an anticline-syncline pair. Initial uplift exposed easily eroded Mesozoic mudstones that were transported through the embryonic growth syncline and deposited farther out in the basin. An average of 6.46 km of uplift and 12.1% of shortening occurred along the range margin during this earliest stage of fault-related fold development. Continued growth syncline development was characterized by uplift and exposure of resistant Paleozoic carbonate rocks. This resulted in deposition of the Fort Union and Kingsbury conglomerates along the hinge of the growth syncline. Fold limb rotation, development of progressive unconformities, reworking of proximal facies along the steeper limb of the syncline, and basinward progradation of alluvial-fan deposits are indicative of this stage. An average of 8.17 km of uplift and 16.9% of shortening had occurred along the range margin by the end of this stage (end of stage I).

(2) The intermediate stage (stage II) of footwall growth syncline development involved partial truncation of the growth syncline by the advancing thrust faults and deposition of the Moncrief Conglomerate. The lower portion of the Moncrief Conglomerate was rotated basinward in the developing growth syncline in a manner similar to that of the Kingsbury Conglomerate during the early stage of deformation.

(3) A final stage of deformation (stage III) along the east-central Bighorn Mountains was characterized by thrust faulting of middle and lower Paleozoic strata over Eocene synorogenic conglomerate. The Moncrief Conglomerate was deformed during this stage of fault-related fold development, when the initially blind thrusts propagated into the near-surface conglomerate deposits, truncated the entire footwall syncline, and overrode the synorogenic conglomerate package. An average of 9.7 km of uplift and 24.1% of short-

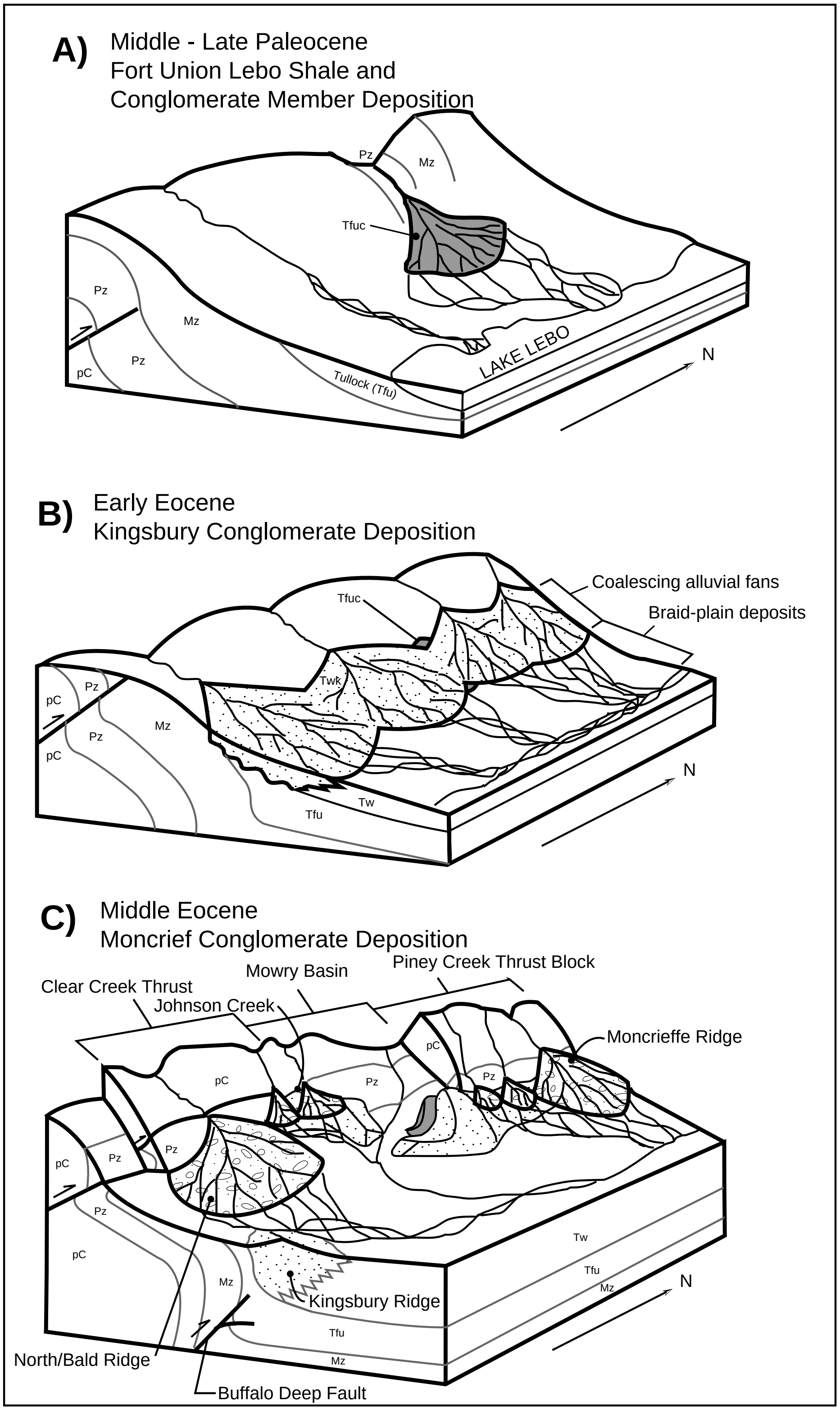

Figure 16. Sequence of schematic block diagrams depicting the depositional and structural history of the east-central Bighorn Mountains. (A) Middle to late Paleocene: Initial uplift along the Bighorn thrust system caused unroofing of Mesozoic mudstones (Mz) and deposition of the Lebo Shale in the Powder River basin. The Fort Union conglomerate (Tfuc) of the Mowry basin was deposited in the late Paleocene when resistant mid-lower Paleozoic strata (Pz) were locally exposed in the hanging wall of the Bighorn thrust. pC—Precambrian rocks. (B) Early Eocene: Regional exposure of lower Paleozoic strata in the hanging wall leads to deposition of the Kingsbury Conglomerate (Twk) along the east-central range margin. Tw—Wasatch Formation. (C) Middle Eocene: Localized shortening resulted in additional displacement along the Clear Creek and Piney Creek thrust faults, exposure of Precambrian rocks (pC) in the hanging wall, and deposition of the Moncrief Conglomerate (open circle pattern) in footwall growth synclines.

ening occurred along the range margin, where this final stage of deformation is well developed.

(4) The type of synorogenic detritus deposited along the eastern margin of the Bighorn Mountains was influenced by source terrane lithology. Initial uplift of the Bighorn Mountains occurred during the early to middle Paleocene and is represented by deposition of the Lebo Shale in the Powder River basin. The Lebo Shale is at least partly the product of unroofing of the Mesozoic mudstones carried in the hanging wall of the Bighorn thrust fault

system. The late Paleocene–Eocene conglomerates do not represent the initiation of Laramide uplift, but instead represent the exposure of coarse-clast–forming rocks in the hanging-wall stratigraphic section.

ACKNOWLEDGMENTS

This study was part of a Master's thesis completed by Hoy at Purdue University. Hoy's graduate studies were supported by Mobil Oil, Geological Society of America, American Association of Petroleum Geologists, Sigma Xi, Colorado Scientific Society, and the Department of Earth and Atmospheric Sciences at Purdue University. Ryan Nichols provided field assistance for Hoy. Ridgway thanks Ron Cole and Peter DeCelles for field work and discussions during the initial stages of this study; Jean Weaver for a field trip that introduced him to the geology of the western Powder River basin; and Jay Scheevel for useful discussions and an aerial tour of the study area. We thank Arvid Johnson for helpful discussions on folds and the many ranch owners for access to outcrops. Recommendations by *Bulletin* reviewers Peter DeCelles, Chris Schmidt, Jim Steidtmann, and Lynn Walter significantly improved the manuscript.

REFERENCES CITED

Anadon, P., Cabrera, L., Colombo, F., Marzo, M., and Riba, O., 1986, Syntectonic intraformational unconformities in alluvial fan deposits, eastern Ebro basin margins (NE Spain), *in* Allen, P., and Homewood, P., eds., Foreland basins: International Association of Sedimentologists Special Publication 8, p. 259–271.

Ayers, W. B., 1986, Lacustrine and fluvial-deltaic depositional systems, Fort Union Formation (Paleocene), Powder River Basin, Wyoming and Montana: American Association of Petroleum Geologists Bulletin, v. 70, p. 1651–1673.

Beck, R. A., Vondra, C. F., Filkins, J. E., and Olander, J. D., 1988, Syntectonic sedimentation and Laramide basement thrusting, Cordilleran foreland: Timing of deformation, *in* Schmidt, C. J., and Perry, W. J., Jr., eds., Interaction of Rocky Mountain foreland and the Cordilleran thrust belt: Geological Society of America Memoir 171, p. 465–487.

Blackstone, D. L., 1981, Compression as an agent in deformation of the east-central flank of the Bighorn Mountains, Sheridan, and Johnson Counties, Wyoming: University of Wyoming Contributions to Geology, v. 19, p.105–122.

Brown, W. G., 1983, Sequential development of the fold-thrust model of foreland deformation, *in* Lowell, J. D., ed., Rocky Mountain foreland basins and uplifts: Denver, Colorado, Rocky Mountain Association of Geologists, p. 57–64.

Brown, W. G., 1988, Deformational style of Laramide uplifts in the Wyoming foreland, *in* Schmidt, C. J., and Perry, W. J., Jr., eds., Interaction of the Rocky Mountain foreland and the Cordilleran thrust belt: Geological Society of America Memoir 171, p. 1–25.

Burbank, D. W., and Vergés, J., 1994, Reconstruction of topography and related depositional systems during active thrusting: Journal of Geophysical Research, v. 99, p. 20281–20297.

Burbank, D. W., Beck, R. A., Raynold, R. G. H., Hobbs, R., and Tahirkheli, R. A. K., 1988, Thrusting and gravel progradation in foreland basins: A test of post-thrusting gravel dispersal: Geology, v. 16, p. 1143–1146.

Burbank, D. W., Vergés, J., Muñoz, J. A., and Bentham, P., 1992a, Coeval hindward and forward-imbricating thrusting in the south-central Pyrenees, Spain: Timing and rates of shortening and erosion: Geological Society of America Bulletin, v. 104, p. 3–17.

Burbank, D. W., Puigdefabregas, C., and Muñoz, J. A., 1992b, The chronology of the Eocene tectonic and stratigraphic development of the eastern Pyrenean foreland basin, northeast Spain: Geological Society of America Bulletin, v. 104, p. 1101–1120.

Curry, W. H., 1971, Laramide structural history of the Powder River Basin, Wyoming, *in* Renfro, A. R., ed., Symposium on Wyoming tectonics and their economic significance: Wyoming Geological Association 23rd Annual Field Conference Guidebook, p. 49–60.

Dahlstrom, C. D. A., 1969, Balanced cross sections: Canadian Journal of Earth Sciences, v. 6, p. 743–757.

Darton, N. H., 1906, Geology of the Bighorn Mountains: U.S. Geological Survey Professional Paper 51, 129 p.

DeCelles, P. G., 1994, Late Cretaceous–Paleocene synorogenic sedimentation and kinematic history of the Sevier thrust belt, northeast Utah and southwest Wyoming: Geological Society of America Bulletin, v. 106, p. 32–56.

DeCelles, P. G., and Mitra, G., 1995, History of the Sevier orogenic wedge in terms of critical taper models, northeast Utah and southwest Wyoming: Geological Society of America Bulletin, v. 107, p. 454–462.

DeCelles, P. G., and 15 others, 1987, Laramide thrust generated alluvial fan sedimentation, Sphinx Conglomerate, southwestern Montana: American Association of Petroleum Geologists Bulletin, v. 71, p. 135–155.

DeCelles, P. G., Gray, M. B., Ridgway, K. D., Cole, R. B., Srivastava, P., Pequera, N., and Pivnik, D. A., 1991, Kinematic history of a foreland uplift from Paleocene synorogenic conglomerate, Beartooth Range, Wyoming and Montana: Geological Society of America Bulletin, v. 103, p. 1458–1475.

DeCelles, P. G., Pile, H. T., and Coogan, J. C., 1993, Kinematic history of the Meade thrust based on provenance of the Belcher Conglomerate at Red Mountain, Idaho, Sevier thrust belt: Tectonics, v. 12, p. 1436–1450.

Demorest, M. H., 1941, Critical structural features of the Bighorn Mountains, Wyoming: Geological Society of America Bulletin, v. 52, p. 161–176.

Dickinson, W. R., Klute, M. A., Hayes, M. J., Janecke, S. U., Lundin, E. R., McKittrick, M. A., and Olivares, M. D., 1988, Paleogeographic and paleotectonic setting of Laramide sedimentary basins in the Rocky Mountain region: Geological Society of America Bulletin, v. 100, p. 1023–1039.

Espina, R. G., Alonso, J. L., and Pulgar, J. A., 1996, Growth and propagation of buckle folds determined from syntectonic sediments (the Ubierna Fold Belt, Cantabrian Mountains, N. Spain): Journal of Structural Geology, v. 18, p. 431–441.

Ethridge, F. G., Jackson, T. L., and Youngberg, A. D., 1981, Floodbasin sequence of a fine-grained meander belt subsystem; the coal bearing lower Wasatch and upper Fort Union Formations, southern Powder River Basin, Wyoming, *in* Ethridge, F. G., and Flores, R. M., eds., Recent and ancient nonmarine depositional environments, models for exploration: Society of Economic Paleontologists and Mineralogists Special Publication 31, p. 191–209.

Fischer, M. P., Woodward, N. B., and Mitchell, M. M., 1992, The kinematics of break-thrust folds: Journal of Structural Geology, v. 14, p. 451–460.

Flemings, P. B., and Jordan, T. E., 1990, Stratigraphic modeling of foreland basins: Interpreting thrust deformation and lithosphere rheology: Geology, v. 18, p. 430–434.

Flores, R. M., 1986, Styles of coal deposition in Tertiary alluvial deposits, Powder River Basin, Montana and Wyoming, *in* Lyons, P. C., and Rice, C. L., eds., Paleoenvironmental and tectonic controls in coal-forming basins of the United States: Geological Society of America Special Paper 210, p. 79–104.

Flores, R. M., and Ethridge, F. G., 1985, Evolution of intermontane fluvial systems of Tertiary Powder River Basin, Montana and Wyoming, *in* Flores, R. M., and Kaplan, S. S., eds., Cenozoic paleogeography of the west-central United States: Denver, Colorado, Society of Economic Paleontologists and Mineralogists, Rocky Mountain Section, p. 107–126.

Flores, R. M., and Hanley, J. H., 1984, Anastomosed and associated coal-bearing fluvial deposits; upper Tongue River Member, Paleocene Fort Union Formation, northern Powder River Basin, Wyoming, U.S.A., *in* Rahmani, R. A., and Flores, R. M., eds., Sedimentology of coal and coal-bearing sequences: International Association of Sedimentologists Special Publication 7, p. 85–103.

Flores, R. M., and Warwick, P. D., 1984, Dynamics of coal deposition in intermontane alluvial paleoenvironments, Eocene Wasatch Formation, Powder River Basin, Wyoming, *in* Proceedings, Geology of Rocky Mountain Coal Symposium, Sixth: North Dakota Geological Society Publication 84-1, p. 184–199.

Foster, N., Goodwin, P. E., and Fisher, R. E., 1969, Seismic evidence for high-angle flank faulting, Bighorn Mountains, Wyoming [abs.]: Geological Society of America Special Paper 121, p. 100–101.

Graham, S. A., and 14 others, 1986, Provenance modeling as a technique for analyzing source terrane evolution and controls on foreland sedimentation, *in* Allen, P. A., and Homewood, P., eds., Foreland basins: International Association of Sedimentologists Special Publication 8, p. 425–436.

Gries, R., Dolson, J. C., and Raynolds, R. G. H., 1992, Structural and stratigraphic evolution and hydrocarbon distribution, Rocky Mountain foreland, *in* Macqueen, R. W., and Leckie, D. A., eds., Foreland basins and fold belts: American Association of Petroleum Geologists Memoir 55, p. 395–425.

Hansley, P. L., and Brown, J. L., 1993, Provenance of the Tullock Member of the Fort Union Formation, Powder River Basin, Wyoming and Montana: Evidence for early Paleocene Laramide uplift: The Mountain Geologist, v. 30, p. 25–34.

Hardy, S., and Poblet, J., 1994, Geometric and numerical model of progressive limb rotation in detachment folds: Geology, v. 22, p. 371–374.

Heller, P. L., and Paola, C., 1992, The large-scale dynamics of grain-size variation in alluvial basins, 2: Application to syntectonic conglomerate: Basin Research, v. 4, p. 91–102.

Heller, P. L., Angevine, C. L., Winslow, N. S., and Paola, C., 1988, Two-phase stratigraphic model of foreland basin sequences: Geology, v. 16, p. 501–504.

Hickey, L. J., 1980, Paleocene stratigraphy and flora of the Clark's Fork Basin, *in* Gingerich, P. D., ed., Early Cenozoic paleontology and stratigraphy of the Bighorn Basin: University of Michigan Papers on Paleontology, v. 24, p. 33–49.

Holl, J. E., and Anastasio, D. J., 1993, Paleomagnetically derived folding rates, southern Pyrenees, Spain: Geology, v. 21, p. 271–274.

Hoppin, R. A., 1961, Precambrian rocks and their relationship to Laramide structure along the east flank of the Bighorn Mountains near Buffalo, Wyoming: Geological Society of America Bulletin, v. 72, p. 351–368.

Hose, R. K., 1955, Geology of the Crazy Woman area, Johnson County, Wyoming: U.S. Geological Survey Bulletin 1027-B, 118 p.

Hoy, R. G., 1996, Laramide tectonics of the east-central Bighorn Mountains, Wyoming: Implications for footwall growth syncline evolution and intraforeland basin development [Master's thesis]: West Lafayette, Indiana, Purdue University, 130 p.

Hoy, R. G., and Ridgway, K. D., 1995, Styles of footwall deformation in Eocene synorogenic conglomerates, east-central flank of the Bighorn Mountains, Wyoming: Geological Society of America Abstracts with Programs, v. 27, no. 5, p. 14.

Hudson, R. F., 1992, Interpretation of the Piney Creek thrust and oil exploration: Wyoming Geological Association 50th Anniversary Field Conference Guidebook, p. 155–166.

Jenkins, C., 1986, A preliminary tectonic analysis of the northeastern margin of the Bighorn Uplift: Buffalo to Dayton, Wyoming [Master's thesis]: Rapid City, South Dakota School of Mines and Technology, 116 p.

Jordan, T. E., Allmendinger, R. W., Dmanti, J. F., and Drake, R. E., 1993, Chronology of motion in a complete thrust belt: The Precordillera, 30–31 °S, Andes Mountains: Journal of Geology, v. 101, p. 135–156.

Jordan, T. E., Flemings, P. B., and Beer, J. A., 1988, Dating thrust-fault activity by use of foreland basin strata, *in* Kleinspehn, K. L., and Paola, C., eds., New perspectives in basin analysis: New York, Springer-Verlag, p. 307–330.

Kellogg, K. S., Schmidt, C. J., and Young, S. W., 1995, Basement and cover-rock deformation during Laramide contraction in the northern Madison Range (Montana) and its influence on Cenozoic basin formation: American Association of Petroleum Geologists Bulletin, v. 79, p. 1117–1137.

Lawton, T. F., 1985, Style and timing of frontal structures, thrust belt, central Utah: American Association of Petroleum Geologists Bulletin, v. 69, p. 1145–1159.

Lawton, T. F., 1986, Compositional trends within a clastic wedge adjacent to a fold-thrust belt: Indianola Group, central Utah, U.S.A., *in* Allen, P. A., and Homewood, P., eds., Foreland basins: International Association of Sedimentologists Special Publication 8, p. 411–423.

Lawton, T. F., Boyer, S. E., and Schmitt, J. G., 1994, Influence of inherited taper on structural variability and conglomerate distribution, Cordilleran fold and thrust belt, western United States: Geology, v. 22, p. 339–342.

Mapel, W. J., 1959, Geology and coal resources of the Buffalo–Lake DeSmet area, Johnson and Sheridan Counties, Wyoming: U.S. Geological Survey Bulletin 1078, 148 p.

McConnell, D. A., 1994, Fixed-hinge, basement-involved fault-propagation folds, Wyoming: Geological Society of America Bulletin, v. 106, p. 1583–1593.

McConnell, D. A., and Wilson, T. G., 1993, Linkage between deformation of basement rocks and sedimentary rocks in basement-involved foreland folds, *in* Schmidt, C. J., Chase, R. B., and Erslev, E. A., eds., Laramide basement deformation in the Rocky Mountain foreland of the western United States: Geological Society of America Special Paper 280, p. 319–333.

Medwedeff, D. A., 1989, Growth fault-bend folding at southeast Lost Hills, San Joaquin Valley, California: American Association of Petroleum Geologists Bulletin, v. 73, p. 54–67.

Merin, I. S., and Lindholm, R. C., 1986, Evidence that the crystalline cores of uplifts adjacent to the Powder River Basin were breached during Paleocene time: The Mountain Geologist, v. 23, p. 128–131.

Mitra, S., 1990, Fault-propagation folds: Geometry, kinematic evolution, and hydrocarbon traps: American Association of Petroleum Geologists Bulletin, v. 74, p. 921–945.

Nelson, R. S., 1968, Tertiary deposits and morphology east flank Bighorn Mountains: Wyoming Geological Association, Earth Science Bulletin, p. 19–24.

Obernyer, S. L., 1979, Basin-margin depositional environments of the Fort Union and Wasatch Formations in the Buffalo–Lake DeSmet area, Johnson County, Wyoming: U.S. Geological Survey Open-File Report 79-712, 116 p.

Palmquist, J. C., 1978, Laramide structure and basement block faulting: Two examples from the Bighorn Mountains, Wyoming, *in* Matthews, V., III, ed., Laramide folding associated with basement block faulting in the western United States: Geological Society of America Memoir 151, p. 125–128.

Pivnik, D. A., 1990, Thrust-generated fan-delta deposition: Little Muddy Creek Conglomerate, SW Wyoming: Journal of Sedimentary Petrology, v. 60, p. 489–503.

Pivnik, D. A., and Khan, M. J., 1996, Transition from foreland- to piggyback-basin deposition, Plio–Pleistocene upper Siwalik Group, Shinghar Range, NW Pakistan: Sedimentology, v. 43, p. 631–646.

Poblet, J., and Hardy, S., 1995, Reverse modeling of detachment folds, application to the Pico del Aguila anticline in the South Central Pyrenees (Spain): Journal of Structural Geology, v. 17, p. 1707–1724.

Ridgway, K. D., Cole, R. B., and DeCelles, P. G., 1991, Unroofing history, alluvial-fan facies, and deformation of Paleogene synorogenic conglomerates, Bighorn Range, Wyoming: Geological Society of America Abstract with Programs, v. 23, no. 5, p. A131.

Ridgway, K. D., DeCelles, P. G., and Cole, R. B., 1992, Influence of Laramide thrusting on Paleogene alluvial-fan conglomerates, Bighorn Range, Wyoming: Society for Sedimentary Geology–Society of Economic Paleontologists and Mineralogists Theme Meeting, Abstracts with Programs, p. 56.

Ridgway, K. D., Trop, J. M., and Sweet, A. R., 1997, Thrust-top basin formation along a suture zone, Cantwell basin, Alaska Range: Implications for development of the Denali fault system: Geological Society of America Bulletin, v. 109, p. 505–523.

Robbins, S. L., and Grow, J. A., 1990, Structural and basement-lithological implication of gravity and seismic-reflection data across the central Powder River Basin from the Black Hills to the Bighorn Mountains [abs.], *in* Carter, L. M. H., ed., U.S. Geological Survey research on energy resources: U.S. Geological Survey Circular 1060, p. 71.

Schmidt, C. J., and 11 others, 1993, Mechanical behavior of basement rocks during movement of the Scarface thrust, central Madison Range, Montana, *in* Schmidt, C. J., Chase, R. B., and Erslev, E. A., eds., Laramide basement deformation in the Rocky Mountain foreland of the western United States: Geological Society of America Special Paper 280, p. 89–106.

Seeland, D. S., 1976, Relationships between early Tertiary sedimentation patterns and uranium mineralization in the Powder River Basin, Wyoming, *in* Laudon, R. B., ed., Geology and energy resources of the Powder River Basin: Wyoming Geological Association 28th Annual Field Conference Guidebook, p. 53–64.

Sharp, R. P., 1948, Early Tertiary fanglomerate, Big Horn Mountains, Wyoming: Journal of Geology, v. 56, p.1–15.

Stearns, D. W., 1978, Faulting and forced folding in the Rocky Mountain foreland, *in* Matthews, V., III, ed., Laramide folding associated with basement block faulting in the western United States: Geological Society of America Memoir 151, p. 1–37.

Steidtmann, J. R., and Middleton, L. T., 1991, Fault chronology and uplift history of the southern Wind River Range, Wyoming: Implications for Laramide and post-Laramide deformation in the Rocky Mountain foreland: Geological Society of America Bulletin, v. 103, p. 472–485.

Steidtmann, J. R., and Schmitt, J. G., 1988, Provenance and dispersal of tectogenic sediments in thin-skinned, thrusted terrains, *in* Kleinspehn, K. L., and Paola, C., eds., New perspectives in basin analysis: New York, Springer-Verlag, p. 353–366.

Stone, D. S., 1993, Basement-involved generated folds as seismically imaged in the subsurface of the central Rocky Mountain foreland, *in* Schmidt, C. J., Chase, R. B., and Erslev, E. A., eds., Laramide basement deformation in the Rocky Mountain foreland of the western United States: Geological Society of America Special Paper 280, p. 271–318.

Suppe, J., 1983, Geometry and kinematics of fault-bend folding: American Journal of Science, v. 283, p. 684–721.

Suppe, J., and Medwedeff, D. A., 1990, Geometry and kinematics of fault-propagation folding: Eclogae Geologicae Helvetiae, v. 83, p. 409–454.

Tewalt, S. J., Baur, M. A., Mathew, D., Roberts, M. P., Ayers, W. B., Jr., Barnes, J. W., and Kaiser, W. R., 1983, Estimation of coal resources in Texas Gulf Coast, Ohio northern Appalachian and Wyoming Powder River basins: A comparison of statistical approaches: University of Texas Bureau Economic Geology Report of Investigations 136, 157 p.

Vergés, J., Burbank, D. W., and Meigs, A., 1996, Unfolding: An inverse approach to fold kinematics: Geology, v. 24, p. 175–178.

Weaver, J. N., and Flores, R. M., 1987, Environments of deposition of Late Paleocene coals, western Powder River Basin, Wyoming, U.S.A., *in* Johnson, D., ed., Advances in coal measure accumulation: Geological Society of Australia Special Publication, p. 121–137.

Wing, S. L., Bown, T. M., and Obradovich, J. D., 1991, Early Eocene biotic and climatic change in interior western North America: Geology, v. 19, p. 1189–1192.

Woodward, N. B., Boyer, S. E., and Suppe, J., 1985, An outline of balanced cross sections: University of Tennessee Department of Geology Studies in Geology, v. 11, 170 p.

Zapata, T. R., and Allmendinger, R. W., 1996, Growth stratal records of instantaneous and progressive limb rotation in the Precordillera belt and Bermejo basin, Argentina: Tectonics, v. 15, p. 1065–1083.

MANUSCRIPT RECEIVED BY THE SOCIETY, APRIL 19, 1996
REVISED MANUSCRIPT RECEIVED, OCTOBER 10, 1996
MANUSCRIPT ACCEPTED DECEMBER 17, 1996

Printed in U.S.A.